2016

Hydraulic system modeling and optimization to achieve performance characteristics

Kathryn Kline
Iowa State University

Hydraulic system modeling and optimization to achieve performance characteristics

by

Kathryn Kline

A thesis submitted to the graduate faculty
in partial fulfillment of the requirements for the degree of

MASTER OF SCIENCE

Major: Agricultural and Biosystems Engineering

Program of Study Committee:
Brian Steward, Major Professor
Stewart Birrell
Steven Hoff

Iowa State University

Ames, Iowa

2016

TABLE OF CONTENTS

LIST OF FIGURES

LIST OF TABLES

ABSTRACT

As automation technology continues to be integrated into industrial and mobile machinery, more precise control of hydraulic cylinders will assist in the achievement of desired response characteristics. Thus, in designing the cushioning mechanism for a hydraulic cylinder, there is value in predicting the deceleration response due to pressure generated when fluid passes through the cushion orifice. The cushion orifice can be designed to change as a function of piston position to meet a desired velocity response. In practice, determination of the orifice area requires a lengthy iterative process of trial and error. Therefore, to overcome these design process challenges, dynamic models of cylinder cushioning systems were developed that, when solved numerically, predicted the pressure and velocity responses of the cylinder with time. Utilizing these dynamic models, a cushion design optimization procedure was also developed to obtain the dimensions of the cushioning spear that most closely obtains the desired velocity response profile. Simulations of the dynamic cushion model were performed using a cushion spear with a shape designed through a static analysis to produce constant deceleration during the cushioning phase. Spear shapes were fit to the analytically developed common spear profile and their performance was assessed with simulation. The developed optimization procedure was run to compare the performance the spear shapes common to industry. Lastly, to identify the range of results produced by the optimizer, the procedure was run ten times for each spear type with the variation between runs. The performance of each run was quantified by measuring the root-mean square error (RMSE) between the desired velocity profile and the simulated velocity profile. When surrounding system conditions were held constant, the analytical analysis produced

a profile leading to nearly constant deceleration with an RMSE of $1.4x10^{-3}$ m/s (0.29 feet per minute; fpm) when simulated by the dynamic model. However, attempts to replicate the results of the analytical model with common spear shapes resulted in deviation from the constant deceleration goal with the parabolic and linear regression curves producing RMSE values of $14.9x10^{-3}$ and $21.7x10^{-3}$ m/s (2.94 and 4.28 fpm) respectively. The optimizer produced a consistent family of results for each spear with an average standard deviation of $2.6x10^{-3}$ m/s (0.51 fpm). This dynamic modeling approach has potential to assist designers in the development of cushioning spears that meet customer cushion response specifications.

CHAPTER 1. GENERAL INTRODUCTION

Introduction

The principles that provide the basis of fluid power were being developed as early as the 1600's (Daines, 2009). However, the hydraulic portion of the fluid power industry, as we know it today, has mainly been developed within the last century, particularly since a hydraulic system utilizing oil instead of water was used to control guns on the USS Virginia in 1906 (Esposito, 2003). The economic impact of the fluid power industry still remains strong today; based on 2013 U.S. Census Bureau data, sales within the fluid power industry surpassed $22 billion and provided jobs for 71,000 people. After taking a broader view of the industry and including ten key industries that utilize fluid power components, the employment numbers increase to over 874,000 people with payroll figures exceeding $54.4 billion (Stelson, 2015).

Figure 1.1: Multiple sectors of industry incorporate fluid power components. (Photo: beisensors.com)

Recent developments in the fluid power industry have focused on the incorporation of sensing and control technology to develop systems that have the potential to increase machine productivity and efficiency. For instance, automating certain machinery such as an agricultural sprayer can allow for more efficient application of agricultural chemicals and a reduced environmental impact. Achieving improvements

in the efficiency and productivity of equipment like the sprayer requires improved motion control of the mechanical systems involved in the machine's operation.

Mechanical motions within machines, like the sprayer, are typically controlled with hydraulic systems instead of pneumatics due to the higher power density of the less compressible hydraulic oil. The motion control provided by these hydraulic systems can be divided into two sub-categories, rotational motion and linear motion. While rotational motion can be generated by hydraulically with motors, linear motion control is typically accomplished using hydraulic cylinders.

While linear motion control can be conducted through alternative methods using mechanical and electrical systems, a hydraulic cylinder's ability to transmit power is limited only by the structural strength of the materials used in machining the cylinder (Merritt, 1967). The immense power and force capabilities of a hydraulic cylinder can, however, be detrimental when the moving piston is permitted to impact the case at the end of stroke. Without measures put in place to decelerate the piston and prevent impact with the end of the case, fatigue damage and subsequent failures can occur if the piston is able to impact the case repeatedly. Beyond fatigue damage, a cylinder can be destroyed if the load being moved generates enough momentum to break the case upon impact.

To address the issues regarding damage and unwanted motion due to impact, hydraulic cylinder cushions have been developed to decelerate the piston and rod assembly as it approaches the end of the stroke (Esposito, 2003). Piston deceleration is achieved by metering the fluid as it exits the cylinder causing a pressure increase in either the cap or rod end, depending on direction of motion (Figure 1.2). By increasing the

pressure in these volumes on the back side of the piston, a force resisting the motion of the piston is developed causing the piston to decelerate.

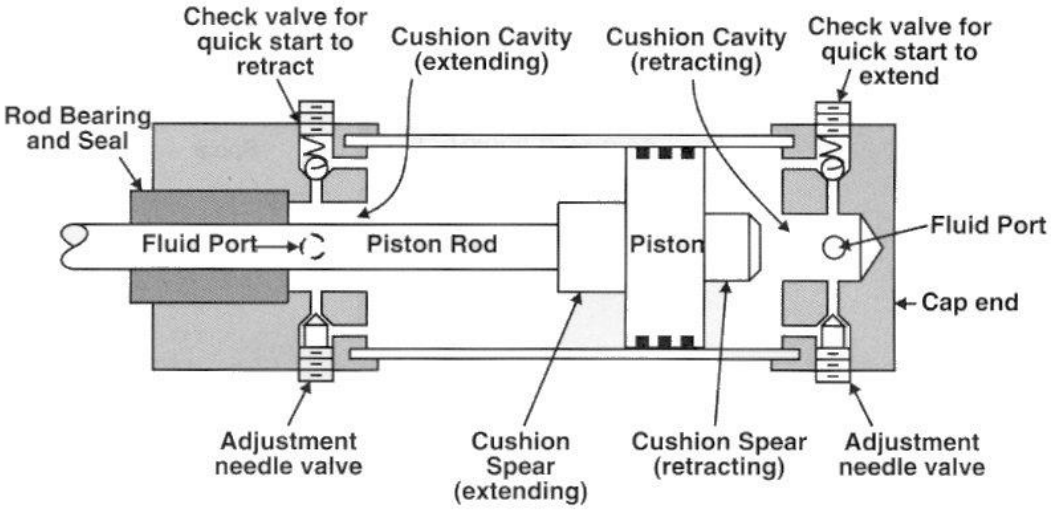

Figure 1.2: Hydraulic cylinder with cushioning spears to meter flow out of fluid port.
(Photo: Norvelle, 1995)

Various approaches to metering the fluid for cylinder cushions have been implemented. One approach diverts the outlet flow through needle valves as the cushion spear enters the cushion cavity (Figure 1.2). An alternative approach utilizes a cushioning spear or collar that either contains a varying outer diameter or internally bored orifices to variably meter the outlet flow as a function of insertion depth of the spear into the cushioning cavity (Anon, 1973). This research project focused on the second approach.

When viewing a cushioning spear from the side or as a cross-section, the varying diameter of the spear utilized in the second approach creates an outline that can be categorized into four different spear shapes: stepped, tapered, parabolic and piccolo (Figure 1.3). The last shape analyzed, the piccolo spear, has a constant external diameter and meters the flow by sequentially covering each of the three fluid ports as the spear enters the cavity.

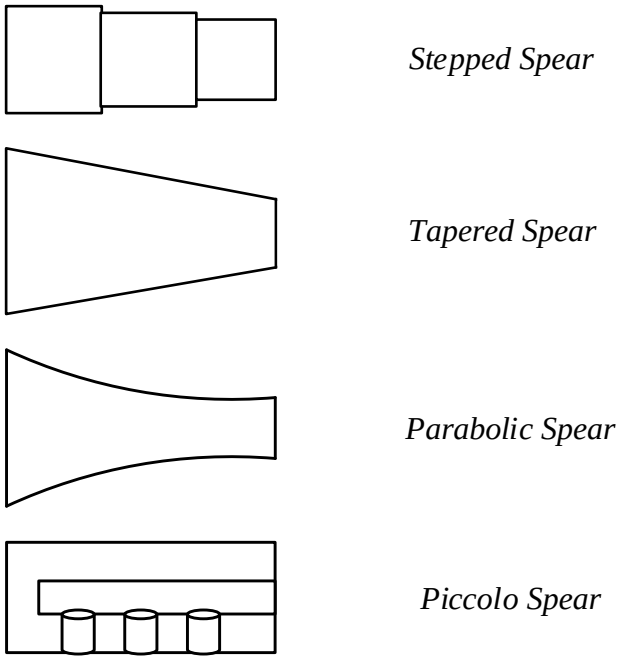

Figure 1.3: Cushion spear profiles with changing cross-sectional area.

Due to the different rate at which the spear diameter increases, each of these designs produces a unique velocity profile as the cylinder decelerates. Therefore, in choosing which of the four designs to implement and selecting the associated dimensional parameters, there is value in being able to predict the effect these design choices will have on the pressure and deceleration response of the cylinder during cushioning.

The objectives of this research are to:

1. Develop a dynamic model that can predict the velocity and pressure performance of a hydraulic cylinder cushion.
2. Support the developed dynamic model through analytical analysis.

3. Utilize the dynamic model to analyze the performance of cushioning spear types commonly found in industry and compare those spears to the analytically developed spear type.
4. Implement a cushion design optimization procedure to find cushioning spear profiles that best achieve a predetermined velocity profile.

Thesis Organization

Following the introductory chapter, the remainder of this thesis is organized through three additional chapters, Chapters 2-4. Chapter 2 presents a review of previous research that was found to be relevant to this project. Chapter 3 describes the mathematical development and results of the dynamic model created to analyze the response of various hydraulic cylinder cushion designs along with the optimization procedure utilized. Chapter 4 presents the conclusions derived at the completion of the project along with suggestions for future research.

References

Anon. "Constant deceleration cylinder has special built-in shock absorber", *Product Engineering*, 1973.

Daines, James R. *Fluid Power: Hydraulics and Pneumatics*. Tinley Park, IL: Goodheart-Willcox, 2009.

Esposito,A. *Fluid Power with Applications* (6th ed.). Upper Saddle River, N.J.: Prentice Hall. 2003.

Merritt, H. *Hydraulic Control Systems*. New York: Wiley, 1967.

Norvelle, F. *Fluid Power Technology*. Minneapolis/St. Paul: West Pub, 1995.

Stelson, Kim. "Engineering research center for compact and efficient fluid power strategic research plan", *Center for Compact and Efficient Fluid Power*, 2015.

CHAPTER 2. LITERATURE REVIEW

Hydraulic cylinders are used extensively in industry to provide linear motion control. These cylinders are composed of cylindrically shaped metal case with a piston-rod assembly (A and B respectively in Figure 2.1) that moves back and forth within the case. The piston and rod assembly separates two different volumes inside the cylinder case. For a single rod cylinder, these two volumes are called: the rod end volume, where the rod end is the end of the cylinder from which the rod protrudes, and the cap end volume, where the cap end does not have a rod (Figure 2.1 c and d respectively). As these volumes are pressurized, hydrostatic forces due to the pressurized fluid act on the surfaces of the vessel containing the fluid. Thus, the forces acting on the piston-rod assembly cause it to move, extending the rod out of the cylinder case or retracting the rod into the cylinder case (Figure 4 shows a cylinder in retraction). An external load can be attached to cylinder rod, and as the piston-rod assembly moves, a force is exerted on the load causing the load to move along a linear path. For a cylinder in retraction, the flow leaving the cap end exits through the cushioning cavity E before returning to the rest of the hydraulic circuit through the cylinder port I. The cylinder stops when the piston reaches the end of its stroke, or when the piston makes contact with the end cap, H. The components labeled F and G are the cylinder cushion spear and collar that decelerate the piston before it contacts the end cap in either retraction or extension, respectively.

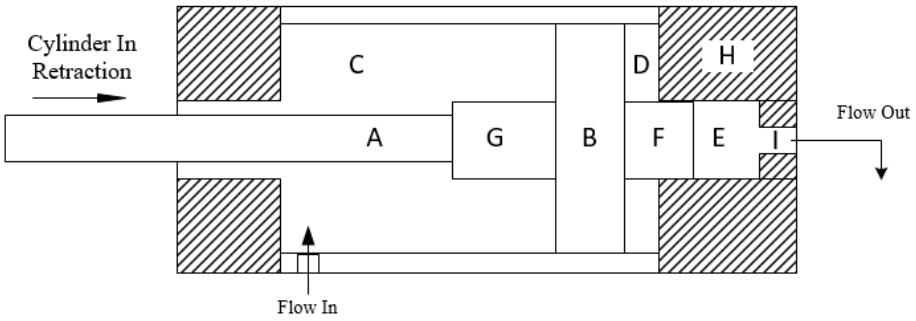

Figure 2.1: Hydraulic cylinder in retraction with main functional components labeled.

Hydraulic cylinders provide high power density for moving heavy loads, but if the cylinders are allowed to reach end of stroke at full speed, sudden deceleration can cause excessive impact (Esposito, 2003). Therefore, a cushioning mechanism was designed to decelerate the cylinder piston and reduce the speed at which impact occurs.

Cylinder cushions meter the flow leaving the cylinder case causing pressure to increase. When the area of the piston is exposed to this accumulating pressure, a force develops that opposes the motion of the piston-rod assembly causing deceleration (Norvelle, 1995). With the importance of accurately metering the fluid leaving the cylinder to create a resisting force, there is value in predicting the pressure response, i.e. the cushion pressure as a function of time, generated when the fluid is metered by the cushioning mechanism orifice.

In approaching the development of a mathematical model to describe the performance of a hydraulic cylinder and cylinder cushion, it was necessary to investigate how other researchers had treated similar systems. In their general approach to describing the system, other researchers seemed to choose one of two methods: an energy based model, or a model based on the principle dynamic equations. The earliest research efforts tended to lean towards the energy approach that required less complicated mathematics.

In more recent investigations, with the assistance of computer-based analysis, numerical simulation provided more insight into the response of the system. The details of how various researchers applied both of these methods, the energy approach and that based on principle equations, were reviewed and are detailed in this chapter.

Additionally, one detail that is often not clear in the published research is the mathematical model used to describe the flow through the annular clearance created by the spear entering the cushioning cavity. The orifice equation appears to be the most utilized model, but there is also a pressure drop as fluid flows through an annular pipe. The insertion depth at which analysis should transition from using one equation to the other is not well identified, so additional research, detailed in this chapter, was conducted to evaluate how critical transitioning between these equations may be.

Modeling a Hydraulic Cylinder Cushion

Previous attempts to model a hydraulic cylinder and simulate the performance of cushioning mechanisms have focused on an energy approach. W.L Green (1968) and John Berninger (1973) both utilized an energy approach to model a hydraulic cylinder cushion while Berninger's approach included additional first principle equations similar to those used during the analysis conducted for the project detailed in this report.

To analyze the effectiveness of a hydraulic cushion design, Green calculated the kinetic energy of the moving piston and concluded whether or not the work done on the piston-rod assembly during cushioning would sufficiently dissipate the energy present in the system (Green, 1968). To conduct his analysis, Green assumed that the hydraulic fluid was incompressible with fully turbulent flow through the cushioning orifice, the seal

friction was negligible, and that there was no remaining energy stored as pressure or fluid velocity remaining after the cushioning orifice.

The kinetic energy of the moving piston was calculated using the known initial velocity of the system, v, and the total mass, m, of the load and the piston-rod assembly (Equation 2.1).

$$KE_0 = \frac{1}{2}mv^2 \tag{2.1}$$

Next the efficiency, η, of the hydraulic cushion was calculated using the mathematical expression:

$$\eta = -\frac{P_M}{P_F}\left(1 - e^{-\lambda}\right) \tag{2.2}$$

where P_M is the maximum allowable cushion pressure,

λ is a dimensionless number described using the mathematical expression:

$$\lambda = \frac{P_M\, A\, L}{KE_0} \tag{2.3}$$

where A is the cross-sectional area of the cushioning spear and L is the length of the cushioning spear,

and P_F is the equivalent static pressure defined by the expression:

$$P_F = \frac{P_E A_1 \pm F}{A} \tag{2.4}$$

where P_E is the maximum system pressure,

A_1 is the effective area of the piston on the driving side, and

F is the external load.

Utilizing the kinetic energy of the moving piston, KE_0, and the cushioning efficiency, η, the kinetic energy remaining after cushioning can be calculated utilizing the expression:

$$KE_L = (1 - \eta)\, KE_0 \tag{2.5}$$

Subtracting the remaining energy from the initial energy present calculates the energy dissipated in cushioning. If all of the remaining energy is assumed to be in the form of kinetic energy, the final velocity of the piston can be calculated by substituting the remaining kinetic energy for the initial kinetic energy in Equation 2.1.

While this approach may predict whether or not a cushion will be effective and calculate certain parameters such as the final velocity, it was not possible to calculate the pressure or velocity response as a function of time. The dynamic model developed for the research described in this thesis utilizes an approach based on principal equations that, when solved numerically, can produce pressure and velocity results over a period of time.

An article written to highlight work conducted by John Berninger compared the pressure response of a hydraulic cylinder cushion utilizing a fixed orifice area to the response of a cushion with an area that varies with stroke distance through the cushioning stage. The fixed area cushion causes a large pressure spike and sudden deceleration while the cushioning orifice with a varying area could cause more gradual pressure increases and deceleration (Anon, 1973). Berninger used an energy approach along with equations developed from first principles to determine the orifice area as a function of the insertion depth of the cushioning spear into the cushioning cavity needed to achieve constant deceleration of the cylinder. Berninger utilized four basic equations (Equations 2.6-2.9).

Newton's second law of motion represented by adding β to work with acceleration terms in g's.

$$F = ma = \frac{W}{g}(\beta g) \tag{2.6}$$

where F is the net force accelerating the piston-rod assembly,

m and a are the mass and acceleration of the piston-rod assembly,

W is the weight of the piston-rod assembly,

g is gravitational acceleration, and

β is a ratio of the piston acceleration rate to the acceleration of gravity.

Bernoulli's equation, which comes from evaluating the conservation of energy within the system, relates the fluid flow velocity through an orifice to the corresponding pressure drop. Mathematically, this relationship is:

$$\frac{\Delta P}{\gamma} = \frac{V_0^2}{2g} \tag{2.7}$$

where ΔP is the pressure drop across the orifice,

γ is the specific weight of the fluid,

V_0 is the velocity of the fluid flowing through the orifice, and

g is gravitational acceleration.

The law of continuity, which is derived from the law of mass conservation, states that all of the flow leaving the case of the cylinder must flow through the cushioning orifice, but that the velocities vary in relation to the different areas. Mathematically, this relationship is:

$$A_2 V_p = C A_0 V_0 \tag{2.8}$$

where A_2 is the piston area minus the cross-sectional area of the cushioning spear,

V_p is the piston velocity,

A_0 and V_0 are the orifice area and flow velocity through the orifice and

C is a flow coefficient that represents the ratio of the stream area at the vena contracta to the orifice area. For round orifices, the minimum flow area, or vena contracta, occurs downstream of the orifice by a length of about half the orifice diameter (Merritt, 1967).

Lastly, Berninger utilized the law of energy conservation to relate the kinetic energy of the system to the potential energy stored in the pressurized fluid and the work being done by the pressurized fluid moving the piston-rod assembly.

$$Work = E_k - E_p \tag{2.9}$$

Berninger developed an equation to find cushion orifice area as a function of cushion spear insertion depth based on the assumption that the inlet and exhaust pressures remain constant. Additional equations not requiring an assumption of constant system pressures have been developed by Berninger, but are proprietary. While Berninger's approach calculates a cushion design with a varying area that will cause a constant rate of

deceleration, there were no equations provided that can calculate the state of the system at various operating points. Additionally no method for calculating the final velocity upon impact with the case was provided.

Schwartz et al. (2005) evaluated the effect of a cushioning collar, or bushing, used to decelerate a hydraulic cylinder in either extension or retraction. In analyzing the hydraulic cylinder, Schwartz utilized the same basic equations as Berninger used including a force balance and an equation derived from the law of mass conservation. Schwartz also included a compressibility factor, so unlike others he did not assume the fluid to be incompressible. To find the pressure drop associated with flow through the cushioning orifice, Schwartz uses an experimentally determined cushioning factor which related the flow through the cushioning orifice to the pressure drop across it which is used in the mathematical relationship:

$$q = f_c\sqrt{\Delta P_c} \tag{2.10}$$

where q and ΔP_c represent the flow through and pressure drop across the cushioning orifice and f_c is the cushioning factor. The complex, changing geometry of the cushioning collar is cited as reasoning for the use of this experimental factor. In addition to modeling the cylinder, with equations derived from Bernoulli's equation, Schwartz developed a model for the proportional directional control valve through which pressurized fluid was supplied to the hydraulic cylinder. Schwartz built a testing apparatus and conducted experiments to validate their model. The reported results of this validation were reported to have a maximum error of 10% between the pressure response of the simulated system and the experimental system.

Chen et al. (2015) and Chengbin et al. (2011) investigated the response of hydraulic cylinder cushions through simulation. To model the flow through the passage created by the cushioning spear entering the cushioning cavity, the simulation software utilized an equation for laminar and turbulent flow through an annular passage. Both Chen and Chengbin validated their results experimentally and achieved a very minimal margin of error. In comparing the peak pressure, the simulated results in the Chen study fell within 3% of the experimentally measured results. Chengbin did not provide quantitative results; but the simulation results were observed to track the experimental results with an error similar to Chen's at 3%. These studies demonstrated that accurate simulations are possible even when certain factors such as fluid leakage and friction are simplified or neglected.

The cited research modeled the cushioning orifice using either the standard orifice equation with a sharp edge or the modified orifice equation for orifices with length.

Modeling Flow through a Cushioning Orifice

While the standard orifice flow and orifice with length equations fit many applications in hydraulics, there is a lack of definition on the maximum length at which the orifice with length equation is valid. Therefore, certain scenarios, such as a hydraulic cylinder with cushion spears and collars, may not be accurately described using the orifice equations. In an attempt to decide which equation best describes the flow through the annular clearance created by a hydraulic cylinder cushion, various flow equations, including those intended for orifices and annular pipes, were evaluated. To have any success in matching results from an annular pipe flow to those generated by the orifice

equation, a nonlinear equation must be used thus eliminating some of the approaches to describing pipe flow.

Kratz et al. (1931) analyzed flow through pipes with an annular cross-section. Their chosen approach utilized the Darcy equation to describe the head loss due to friction. The Darcy equation is a nonlinear relationship between head loss, which is another way to represent pressure drop, and fluid velocity that corresponds to the orifice equation's nonlinear relationship between flow and pressure drop, shown as:

$$h = f\frac{lv^2}{2gm} \tag{2.11}$$

where h is the head loss due to friction,

f is the friction factor,

l is the effective length of the pipe,

m is the mean hydraulic radius,

v is the average fluid velocity, and

g is the acceleration of gravity.

The mean hydraulic radius, m, for an annular pipe is equal to one-fourth of the difference between the diameter of the outer pipe and the diameter of the inner pipe. The friction factor, f, is a function of the roughness of the pipe surface and Reynold's number for the flow.

Merritt (1967) describes an equation for viscous, or laminar, flow through an annular pipe similar to that analyzed by Kratz et. al. However, Merritt's equation presented a linear relationship between the fluid flow and pressure drop, shown as:

$$Q = \frac{\pi r c^3}{6\mu L}\Delta P \tag{2.12}$$

where r is the radius of the cushioning cavity,

c is the clearance between the cushion spear and the wall of the cushioning cavity,

μ is the dynamic viscosity of the fluid,

L is the length of the cushion spear that is inserted into the cushioning cavity, and

ΔP is the pressure drop across the annular clearance.

An additional equation expands on Merritt's work by modeling inertial, or turbulent flow through an annular pipe (Anon, 2013). This equation represented a non-linear relationship between the pressure drop corresponding to flow through the annular clearance, mathematically expressed as:

$$Q = \pi(r^2 - (r-c)^2)\sqrt{\frac{2\Delta P}{\rho}\left(\frac{2c}{\varepsilon L} + \frac{1}{1.5^2}\right)} \tag{2.13}$$

where ρ is the density of the fluid, and

ε is expressed mathematically as:

$$\varepsilon = \frac{0.316}{Re^{0.21}} \tag{2.14}$$

where Re is the Reynolds number of the moving fluid.

When compared to the linear relationship proposed in Merritt, the non-linearity of the equation presented in Anon generated results more aligned to the standard orifice equation when compared to the linear relationship proposed in Merritt.

The studies on modeling a hydraulic cushion have shown that modern modeling techniques utilizing numerical solvers can produce experimentally validated results. Additionally, their success in modeling a hydraulic cylinder supports their assumption that the neglected effect of friction does not substantially impact the accuracy of the results. The studies on orifices flow show that a variety of methods exist to describe the flow through, and pressure drop across, an orifice. With the case of the annular clearance created by the hydraulic cylinder cushion, the definitions of the established orifice flow equations overlap making it difficult to choose the correct equation. Therefore, the equation most relevant to the cushioning clearance being modeled, the annular flow equation, was chosen.

References

Anon. "Constant deceleration cylinder has special built-in shock absorber." *Product Engineering* (1973).

Anon. “Modeling of hydraulic systems.” *Modelon AB* (2013).

Chen, X., J. Zhou, L. Li, and Y. Zhang. "Cushioning structure optimization of excavator arm cylinder." *Automation in Construction* 53 (2015): 120-30.

Chengbin, W., and Q. Long. "Study on simulation and experiment of hydraulic excavator's work device based on Simulation X." *International Conference on Electric Information and Control Engineering, 15-17 April 2011*.

Esposito, A. *Fluid Power with Applications* (6th ed.). Upper Saddle River, N.J.: Prentice Hall, (2003).

Green, W. L. "Cushioning for hydraulic cylinders." *Hydraulics & Pneumatics* (1968): 100-04.

Kratz, A., H. Macintire, and R. Gould. “Flow of liquids in pipes of circular and annular cross-sections.” *University of Illinois Engineering Experiment Station* (1931).

Merritt, H. *Hydraulic control systems*. New York: Wiley, (1967).

Norvelle, F. *Fluid power technology*. Minneapolis/St. Paul: West Pub, (1995).

Schwartz, C., V. J. De Negri, and J. V. Climaco. "Modeling and analysis of an auto-adjustable stroke end cushioning device for hydraulic cylinders." *J. Braz. Soc. Mech. Sci. Eng.* 27.4 (2005): 415-25.

CHAPTER 3. HYRAULIC SYSTEM MODELING AND OPTIMIZATION TO ACHIEVE PERFORMANCE CHARACTERISTICS

Kathryn Kline, Brian L. Steward

Abstract

As automation technology continues to be integrated into industrial and mobile machinery, more precise control of hydraulic cylinders will assist in the achievement of desired response characteristics. Thus, in designing the cushioning mechanism for a hydraulic cylinder, there is value in predicting the deceleration response due to pressure generated when fluid passes through the cushion orifice. In practice, determination of the orifice area requires a lengthy iterative process of trial and error. Therefore, to overcome these design process challenges, dynamic models describing cylinder cushioning systems were developed that, when solved numerically, predict the pressure and velocity responses of the cylinder with time. Simulations of the dynamic cushion model were performed using a cushion spear with a shape designed through an analytical analysis with the intent to produce constant deceleration during the cushioning phase. Due to the uncommon shape developed through the analytical process, spear shapes more common to industry were fit to the analytically developed spear profile and their performance was assessed with simulation. The analytical analysis produced a profile leading to nearly constant deceleration with an RMSE of $1.4x10^{-3}$ m/s (0.29 feet per minute; fpm) when simulated by the dynamic model. However, attempts to match the results of the analytical model with spear shapes more common to industry resulted in deviation from the constant deceleration goal with the parabolic and linear regression curves producing RMSE values of $14.9x10^{-3}$ and $21.7x10^{-3}$ m/s (2.94 and 4.28 fpm) respectively. This means the performance of the cushion is highly sensitive to variations in the spear shape

profile and, to achieve constant deceleration during cushioning, manufacturers must have the capability to produce a spear shape that may not conform to any of the commonly utilized spear shapes. However, when the analytically developed spear profile was simulated with viscous effects the RMSE value increased to $40.7x10^{-3}$ m/s (8.01 fpm) therefore an optimization procedure was developed to select the ideal cushion dimensions with viscous effects included. The optimization procedure produced a consistent family of results for each spear with an average standard deviation of $2.6x10^{-3}$ m/s (0.51 fpm). This dynamic modeling approach has potential to assist designers in cushioning spear development that meets customer cushion response specifications.

Introduction

Modern innovations in the hydraulics industry have revolutionized our ability to automate processes in the agricultural, construction, and manufacturing sectors. Through the application of automation technology, more efficient and less wasteful practices can be implemented. To achieve these advances, automated machines must have hydraulic systems that can provide precise and reliable motion control. Hydraulic systems can control both the rotational and linear motion utilized in these processes. Hydraulic motors are used to implement rotational motion, while linear control is performed by hydraulic cylinders. The focus of this study was to analyze a cushioning component within hydraulic cylinders and to understand the dynamic relationships within the cylinder in an effort to predict and optimize the deceleration performance of the cylinder.

While hydraulic cylinders provide high power density for moving heavy loads, if the cylinders are allowed to reach end of stroke at full speed, particularly with high inertial loads, the sudden deceleration can cause excessive impact (Esposito, 2003).

Therefore, cylinder cushioning technology has been developed with a goal of decelerating the cylinder piston and reducing the speed before the piston-rod assembly reaches the end of stroke.

Cylinder cushions work by metering the flow leaving the cylinder case when the piston-rod assembly nears the end of a stroke. When the fluid flow is restricted, an increase in the cylinder end pressure develops – in the cap end for the retraction stroke and the rod end for the extension stroke. When the piston area is exposed to this increased pressure, a force develops that opposes the motion of the piston-rod assembly, causing it to decelerate (Norvelle, 1995). With the importance of accurately metering the fluid leaving the cylinder to create a resisting force, there is value in predicting the pressure response, i.e. the cushion pressure as a function of time, generated when the fluid is metered by the cushioning mechanism orifice.

Previous attempts to predict the pressure response of a cylinder in deceleration, and the performance of a particular cushioning mechanism, have involved approaches based on both energy conservation and dynamic relationships. Green (1968) and Anon (1973) utilized an energy approach to model the effectiveness of a hydraulic cushion by analyzing if the work done on the piston-rod assembly during cushioning will sufficiently dissipate the kinetic energy of the moving piston, rod and load. Schwartz et al. (2005) evaluated the effect of a cushioning collar, or bushing, instead of a cushioning spear. To predict the pressure and velocity response of the system, Schwartz used a cushioning factor that was estimated from experimental data including the pressure drop across and flow rate through the cushioning orifice. Chen et al. (2015) and Chengbin et al. (2011) analyzed hydraulic cylinder cushions through the use of dynamic system modeling and

simulation. Both Chen and Chengbin validated their results experimentally and achieved results with a margin of error around 3%.

Due to the difficulty of modeling the friction within a system, simulations typically either consider friction within the cylinder negligible or the effect of internal friction is estimated as a small percentage of the load. The results achieved by Chen and Chengbin's investigations demonstrated that accurate simulations are possible even when certain factors such as the friction or fluid leakage are simplified or neglected.

The objectives of this research were to:

1. Compare the cushioning velocity profile produced by the analytically developed spear shape design to those produced using standard spear shapes more commonly used in industry.
2. Investigate the velocity profile and deceleration performance of the four commonly-used spear shapes with dimensions determined by a cushion design optimization procedure.

Methods

The research described in this paper investigated dynamic models that, when solved numerically, simulate the pressure and velocity response of the cylinder. Utilizing the developed dynamic model, a cushion design optimization process was implemented to find cushion designs that will best meet desired velocity response profiles specified by end users. To better understand the fidelity of the dynamic model, tests were run to compare the results of the dynamic model to the expected results of the cushion design produced through an analytical analysis based on a method utilized by Berninger (Anon,

1973). Additional tests were run to evaluate the effectiveness of the optimizing procedure and to compare the performance of various common cushion shapes used in industry. Specifically, a dynamic model was developed in Matlab and analysis was done to find a cushion spear geometry that should result in contact deceleration. Additionally, the cushion design optimization approach was implemented using a genetic algorithm. Tests were also run to support the research objectives.

Development of Cylinder Cushion Dynamic Model

When developing the dynamic model, the cushioning process was broken up into the two main influences that effect the performance of the cushion. The first factor, considered to have the most impact on deceleration, is the orifice created by the cushion spear entering the cylinder cushion cavity (Figure 3.1). The second factor that may have a reasonable impact on the system is the effect of the viscous resistance within the annular passage created by the cushioning spear as it enters the cushioning cavity through which the fluid exits the cylinder.

Additionally, the capacitance of the fluid was included in the model to increase fidelity. The fluid capacitance relates to the pressure spike caused by the sudden metering of the fluid. Originally, with no capacitance included, the model predicted that these pressure spikes could reach levels 2-3 times larger than the operating pressure. However, by adding a relationship describing the system's fluid capacitance, the pressure spikes were either eliminated or replaced with a period of transitory oscillation depending on the style of the cushioning spear.

To develop the equations describing the cylinder cushioning system, the path of the fluid through the system and the corresponding fluid resistances encountered were modeled. Using this approach, the pressure at or fluid flow rate through a specific component in the system can be calculated. An analysis of the system and the included resistances is described below beginning with the development of the flow leaving the cap end of a cylinder. Like electrical resistance is used to relate voltage drop across a resistor to the current going through the resistor through Ohm's law, fluid resistance relates the pressure drop across a hydraulic component to the volume flow rate going through it. For an orifice, valve, fitting or turbulent flow through a fluid conduit, the pressure drop is proportional to the square of the volume flow rate, and fluid resistance is the coefficient of proportionality. For laminar flow through a fluid conduit, pressure drop is proportional to volume flow rate, and fluid resistance is again the coefficient of proportionality. Fluid resistances are calculated based on component geometry and fluid properties.

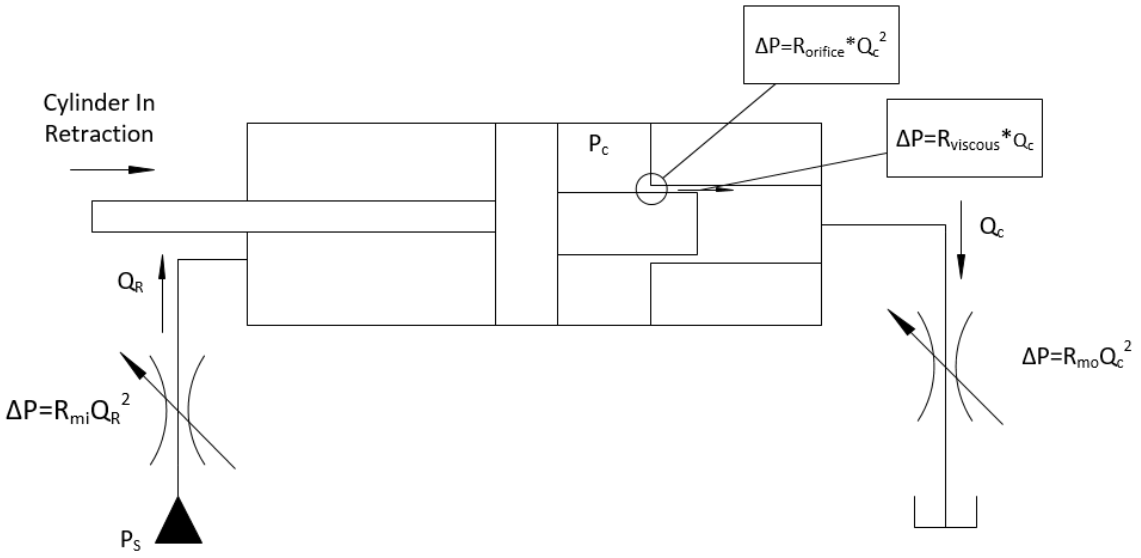

Figure 3.1: Resistances encountered as fluid flows into and out of the cylinder during the cushioning phase of the retraction stroke.

Three resistances are encountered as the fluid leaves the cap end of the cylinder. First, the fluid passes through an orifice, then through the narrow passageway created between the spear and the cavity which causes a viscous resistance to develop in the laminar flow, and finally though a meter out orifice that is included to represent the directional control valve that directs the flow to and from the cylinder. Modeling the cylinder cushion system started at the cap end by summing the pressure drops developed by flow encountering three fluid resistances in series (Figure 3.1). The two orifices create a non-linear relationship between pressure and flow while the viscous resistance remains linear due to the laminar flow through the narrow passageway. The summation of pressure drops is equal to the cap end pressure, which stated mathematically is:

$$P_c = R_{mo}Q_c^2 + R_{orifice}Q_c^2 + R_{viscous}Q_c \tag{3.1}$$

The equation can be rearranged to represent a standard quadratic equation in terms of the fluid flow rate exiting the cap end, Q_c.

$$0 = \left(R_{mo} + R_{orifice}\right)Q_c^2 + R_{viscous}Q_c - P_c \tag{3.2}$$

where R_{mo} is the resistance of the metering orifice located after the outlet of the cylinder,

$R_{orifice}$ is the resistance and the orifice created when the cushioning spear enters the cushioning cavity,

$R_{viscous}$ is the resistance due to laminar flow along the length of the spear as it enters the cushioning cavity, and

P_c is the pressure in the cap end of the cylinder.

This equation can now be solved for fluid flow out of the cap end using the quadratic formula.

$$Q_c = \frac{-R_{viscous} + \sqrt{{R_{viscous}}^2 + 4P_c(R_{mo} + R_{orifice})}}{2(R_{mo} + R_{orifice})} \tag{3.3}$$

The resistance of the meter out valve can be derived from the orifice equation which is:

$$Q = A_{mo} C_D \sqrt{\frac{2(P_c)}{\rho}} \tag{3.4}$$

Rearranging equation 3.4 results in

$$P_c = \frac{\rho}{2A_{mo}^2 c_d^2} Q_c^2 = R_{mo} Q_c^2 \tag{3.5}$$

where ρ is the density of the fluid,

C_d is the discharge coefficient determined by the shape of the orifice, and

A_{mo} is the area of the orifice representing the metering valve.

Similarly, the resistance of the orifice created by the cushioning spear can be derived:

$$R_{orifice} = \frac{\rho}{2A_x^2 C_d^2} \tag{3.6}$$

where A_x is the annular area between the spear and the cushion cavity at the cavity entrance and is defined mathematically as:

$$A_x = \frac{\pi}{4}({d_{cav}}^2 - {d_{cur}}^2) \tag{3.7}$$

d_{cav} is the inside diameter of the cushion cavity into which the cushion spear is inserted, and

d_{cur} is the outside diameter of the cushion spear at the distance from the end of the spear equivalent to the current spear insertion depth.

The diameter, $d_{cur,}$ varies with the insertion depth of the spear, x, and is based on the spear design. Equations to describe this changing diameter were developed for stepped and tapered spears along with the inverted parabola shaped spear (Figure 3.2).

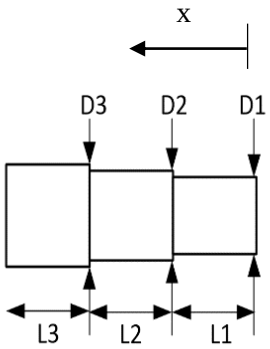

For 0 < x < L1

$$d_{cur} = D1$$

For L1 < x < L2

$$d_{cur} = D2$$

For L2 < x < L3

$$d_{cur} = D3$$

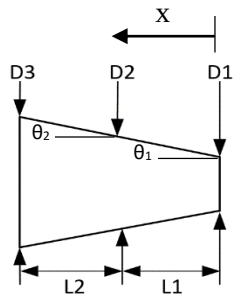

For 0 < x < L1

$$d_{cur} = D1 + 2(x)tan(\theta_1)$$

For L1< x < L2

$$d_{cur} = D2 + 2(x - L1)tan(\theta_2)$$

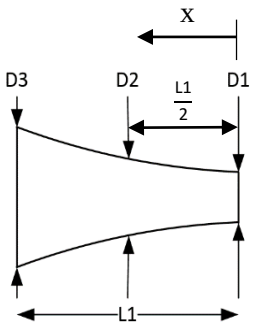

$$d_{cur} = 2\left[\frac{2D_1 - 4D_2 + 2D_3}{L_1^2}x^2\right] + 2\left[\frac{-3D_1 + 4D_2 - D_3}{L_1}x + D_1\right]$$

Figure 3.2: Equations developed to describe the cross-sectional diameter as a function of spear length for (a) a stepped cushion, (b) a two-taper cushion, and (c) a parabolic profile cushion.

Laminar flow will occur in the clearance between the cushion spear and the cavity wall. The associated fluid resistance is also dependent on the calculation of spear diameter at the current insertion depth, d_{cur}. Two fluid resistance relationships as functions of spear insertion depth were needed due to differences in the spear geometries. One equation was derived for the stepped cushion design where the clearance between

the cavity wall and the spear was constant for each step. A second equation was then needed for the tapered and parabolic spear shapes where the clearance varied. The fluid resistance associated with laminar flow through a cylindrical annular geometry can be found from the annular flow equation (Merritt, 1967):

$$\Delta P = \frac{6\mu x Q}{\pi r c^3} \tag{3.8}$$

where

μ is the dynamic viscosity of the hydraulic fluid,

x is the length of the annular passageway,

Q is the flow through the annular passageway,

r is the radius of the outer cylinder, and

c is the clearance between the outer cylinder and the concentric inner cylinder that form the annular passage.

For constant clearance for each step of the stepped spear, when this equation was solved for fluid resistance, the fluid resistance is:

$$R_{viscous\ stepped} = \frac{6\mu x}{\pi \frac{d_{cav}}{2}(d_{cav} - d_{cur})^3} \tag{3.9}$$

where x is the insertion depth of the spear as specified in Figure 3.2. The fluid resistance associated with the tapered and parabolic spear shapes in which the clearance was changing was derived from the same annular flow equation, using infinitesimal annular passageway lengths and integrating of the insertion length of the spear. This analysis resulted in:

$$R_{viscous\ tapered/parabolic} = \frac{6\mu}{\pi\frac{dcav}{2}}\left(\frac{-8x(D_1+xtan(\theta)-dcav)}{(D_1-dcav)^2(D_1+2xtan(\theta)-dcav)^2}\right) \quad (3.10)$$

where θ is the angle of taper on the tapered spear or the angle of taper on the parabola as approximated by taking three evenly spaced points along the spear and calculating the two angles between.

An approach similar to that used for calculating the flow leaving the cap end was utilized to describe the flow into the rod end of the cylinder, Figure 3.1. Summing the pressure drops from system pressure to the pressure in the cylinder rod end.

$$P_R = P_s - R_{mi}{Q_R}^2 \quad (3.11)$$

where R_{mi} is the resistance of the meter-in valve.
Solving for the flow rate into the cylinder rod end.

$$Q_R = \frac{\sqrt{P_s - P_R}}{R_{mi}} \quad (3.12)$$

Applying Newtons's second law to the cylinder piston, rod, and load assembly results in the relationship:

$$ma = P_R(A_p - A_R) - P_C A_{Pcush} - C_t v + mgcos(\theta_m) \quad (3.13)$$

where P_R is the rod end pressure,

A_p is the cross-sectional area of the piston,

A_R is the cross-sectional area of the rod,

A_{Pcush} is the cross-sectional area of the piston with the cross-sectional area of the cushioning cavity removed,

m is the mass of the piston-rod assembly along with the mass of an applied load,

C_t is the viscous damping coefficient representing internal friction in the cylinder, and θ_m is the mounting angle of the cylinder relative to vertical.

Equation 3.13 was rearranged to solve for the acceleration of the cylinder piston, rod, and load assembly which can be written as the time derivative of velocity resulting in:

$$\frac{dv}{dt} = \frac{P_R(A_p - A_R) - P_C A_{Pcush} - C_t v + mgcos(\theta_m)}{m} \tag{3.14}$$

The pressure in either end of the cylinder is developed through the compression of fluid in those volumes. This physical relationship between fluid flow into a volume and the resulting changes in pressure is described by the capacitance equation for the volume at the cap end of the cylinder:

$$\frac{dP_C}{dt} = \frac{A_p v - Q_c}{C_{f_c}} \tag{3.15}$$

and the volume at the rod end of the cylinder:

$$\frac{dP_R}{dt} = \frac{Q_R - (A_p - A_R)v}{C_{f_R}} \tag{3.16}$$

where v is the velocity of the piston, and

C_{fc} and C_{fR} are the fluid capacity of the cap and rod end volumes, respectively.

Fluid capacitance is defined generally as:

$$C_f = \frac{V}{\beta} \tag{3.17}$$

where β is the bulk modulus of the fluid, and

V is the volume of the container holding the fluid (Kulakowski et al., 2007).

For the model, the volume used to calculate the cap end capacitance, C_{fc} was held constant at the length of the cushion spear times the area of the piston to represent the

fluid volume when cushioning begins. For the rod end capacitance C_{fR}, the volume used was calculated as the stroke length of the cylinder minus the length of the cushion and an estimated piston thickness. The volumes were defined this way because the capacitance of the system has the greatest impact on the system dynamics at the start of the cushioning phase.

In the end, the dynamic model of the cylinder cushioning system during retraction consisted of a system of four state equations with v, x, P_c, and P_R as the state variables (Figure 3.3). The rod and cap end flow rates, Q_c and Q_R, were calculated using equations 3.3 and 3.12 for the retracting cylinder. Matlab script was developed to solve this system of equations using the ode45 function, which is a numerical solver utilizing the explicit Runge-Kutta (4,5) formula, called the Dormand-Prince pair (Shampine, 1997). The model was first simulated for three seconds in a pre-cushioning state with $R_{viscous}$ and $R_{orifice}$ set to zero. This step was done to determine the initial conditions when cushioning started. The value of the state variables at the end of the pre-cushioning state were used as the initial conditions for the cushioning stage simulation.

$$\frac{dv}{dt} = \frac{P_R(A_p - A_R) - P_C A_{Pcush} - C_t v + mgcos(\theta_m)}{m}$$

$$\frac{dx}{dt} = v$$

$$\frac{dP_c}{dt} = \frac{A_p v - Q_c}{C_f}$$

$$\frac{dP_R}{dt} = \frac{Q_R - (A_p - A_R)v}{C_f}$$

Figure 3.3: The final system of state equations describing the dynamics of the system.

An additional style of cushioning spear used in industry is the piccolo spear (Anon, 1973). The piccolo spear has a continuous external diameter with a hole bored through the spear axial center and multiple small holes drilled through the sides of the spear through which orifice flow can pass. As the spear enters the discharge port, the holes in the side of the spear are gradually cut off increasing the metering resistance of the exiting fluid (Figure 3.4).

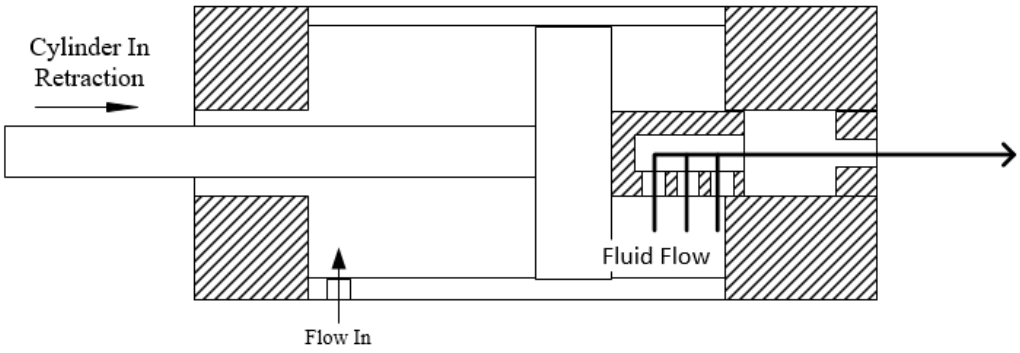

Figure 3.4: Cylinder with a piccolo style cushioning spear (spear shown as a cutaway).

For the piccolo spear, fluid flow takes one of two parallel paths. The fluid leaving the cylinder's cap end either flows through the three piccolo holes and out through the discharge port or the fluid moves through the annular clearance between the piccolo spear and the wall of the cushioning cavity. These two paths were modeled as two sets of fluid resistances in parallel (Figure 3.5).

The upper path with three parallel orifices represents the fluid flowing through the three piccolo holes and out through the discharge port. The lower path represents the flow through the annular clearance and this flow was treated similarly to the annular flow analyzed for the previous spear shapes.

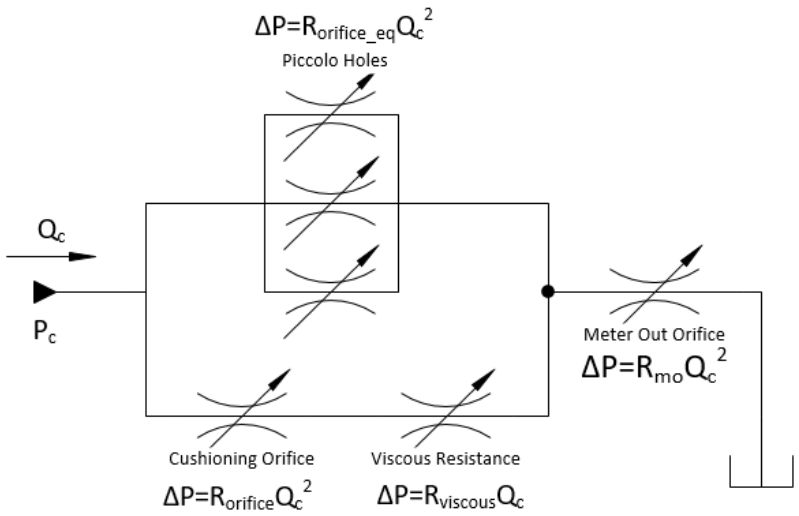

Figure 3.5: Conceptualized flow path with resistances.

Due to the consistent outer diameter of the piccolo spear, the clearance value used in $R_{orifice}$ and $R_{viscous}$ for the lower branch was constant at d_{cav}-d_{cur}. Alternatively, for the upper branch, the effective area of the piccolo holes varies with the insertion depth of the spear (Figure 3.6).

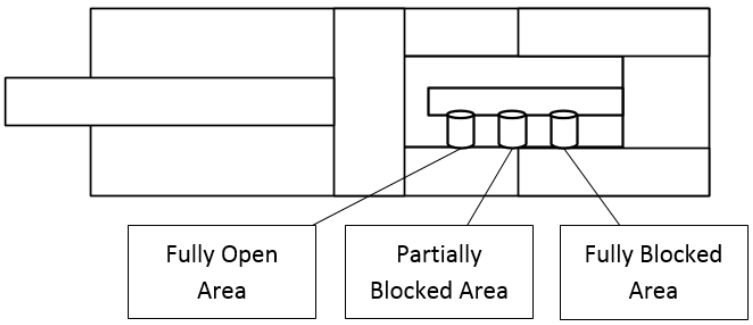

Figure 3.6: Piccolo spear with orifices fully blocked, partially blocked and open.

The flow through each of the three piccolo holes was calculated based on the status of the orifice opening, whether it was open, partially blocked or closed. For a fully open case, the previously used orifice resistance equation was used.

$$R_{orifice} = \frac{\rho}{2A_{px}^2 C_d^2} \tag{3.6}$$

where A_{px} is the area of the orifices bored through the side of the piccolo spear.

If the orifice is fully blocked, the resistance calculation becomes undefined as A_{px} goes to zero, so it is removed from the calculation at this point. The final case, representing a partially blocked orifice, requires an additional equation for the area of a circular port as a function of the portion covered (Manring, 2005).

$$A_x = \frac{\pi}{8}D^2 + \left(\varepsilon - \frac{D}{2}\right)\sqrt{(D-\varepsilon)\varepsilon} + \frac{D^2}{4}\sin^{-1}\left(\frac{2\varepsilon}{D} - 1\right) \tag{3.18}$$

where

D is the diameter of the orifices bored into the sidewall of the spear, and

ε is the length of circular opening that is uncovered.

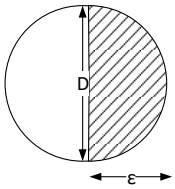

Figure 3.7: Partially blocked orifice, the remaining open area is shown with shading (Manring, 2005).

Finally, because parallel branches in a fluid system must have an equal pressure drop across each branch, the pressure drops across each branch can be set equal to one another.

$$P_c = R_{orifice\_eq}Q_1^2 = R_{orifice}Q_2^2 + R_{viscous}Q_2 \tag{3.19}$$

where Q_1 and Q_2 represent the flow through the upper and lower branch respectively, and

$R_{orifice\_eq}$ is the combined resistance of the three parallel orifice resistances mathematically represented as:

$$R_{orifice\_eq} = \left[\frac{1}{\sqrt{R_{orifice1}} + \sqrt{R_{orifice2}} + \sqrt{R_{orifice3}}}\right]^2 \tag{3.20}$$

where $R_{orifice1}$, $R_{orifice2}$, and $R_{orifice3}$ equal the resistances of each of the three piccolo holes shown in Figure 3.5.

Solving for Q_1, Q_2, and the combined flow rate leaving the cap end, Q_c.

$$Q_1 = \sqrt{\frac{\Delta P}{R_{orifice\_eq}}} \tag{3.21}$$

$$Q_2 = \frac{-R_{viscous} + \sqrt{R_{viscous}^2 - 4R_{orifice}(\Delta P)}}{2R_{orifice}} \tag{3.22}$$

$$Q_c = Q_1 + Q_2 \tag{3.23}$$

where ΔP is the pressure drop between the cap end pressure and the pressure in the cushioning cavity.

The remaining equations defining the state of the system, shown in Figure 3.3, do not need to be altered for the piccolo spear.

An additional model was developed to simulate a cylinder in extension. This model was very similar to the retraction model with variations focused on changing the location where the cushioning spear is inserted from the discharge port to the case. This research project was focused on cylinder in retraction, but similar results are expected for a cylinder in extension.

Analytical Development of Cushion Orifice Area Profile for Constant Deceleration

An analytical approach was used to find cushion orifice area profiles which theoretically should result in constant deceleration. These profiles were then simulated using the dynamic cushion model described above. This analytical approach was pursued to provide confidence in the results of the dynamic model by entering the area profile into

the dynamic model and comparing the resulting velocity profile with that expected from constant deceleration.

The method used for analysis was inspired by work done by John Berninger (Anon, 1973). Berninger presented an analytical approach to calculate the orifice area as a function of cushion insertion depth which would produce a constant deceleration during cylinder cushioning. What was most intriguing and useful about Berninger's approach is that the constant deceleration constraint transforms the differential equations describing cushioning dynamics to an algebraic equation. The constant deceleration constraint based on the idea that, in industry, the ideal cylinder cushion will have a smooth, constant rate of deceleration. This performance is ideal because jolting during the deceleration of a cylinder, perhaps operating an excavator boom, could be felt by the operator causing a distraction. Through applying this constraint, when summing the forces on the cylinder piston-rod assembly, the acceleration can be set to a constant value and the equation becomes algebraic. Mathematically, this is represented as:

$$P_r\left(A_p - A_r\right) - P_c A_p + W = m a_c \tag{3.24}$$

where

P_r is the rod end pressure,

P_c is the cap end pressure,

A_r and A_p are the areas of the piston and rod respectively,

W is the weight of the piston-rod assembly along with any externally mounted load,

m is the mass of the piston-rod assembly along with any load applied to the cylinder, and

a_c is the constant cylinder deceleration.

which, when solved for the cap end pressure becomes:

$$P_c = \frac{1}{A_p}\left[P_R\left(A_p - A_R\right) + W - ma_c\right] \tag{3.25}$$

Next the orifice equation is used to calculate the orifice area that will produce the cap pressure required for constant deceleration from equation 3.24.

$$A_0 = \frac{Q_c}{C_D\sqrt{\frac{2(P_C - P_e)}{\rho}}} \tag{3.26}$$

where

P_e is the exhaust pressure in the discharge port,

C_D is the discharge coefficient based on the geometry of the orifice, and

ρ is fluid density.

Both pressures, the discharge coefficient, and the fluid density are constant. The cap end flow rate, Q_C, is equal to the piston velocity multiplied by the piston area, since the fluid is assumed to be incompressible. The piston velocity is changing with time since the piston-rod assembly is being decelerated, so based on basic physics, the cap end flow rate as a function of time is mathematically:

$$Q_c(t) = v(t)A_p = (a_c t + v_0)A_p \tag{3.27}$$

where v(t) is the piston velocity at time t, and

v_o is the initial velocity of the piston upon the beginning of the cushioning region. Substituting equations 3.25 and 3.27 into equation 3.26 provides an equation for the orifice area as a function of time, t, from the start of the cushioning phase of the retraction stroke.

$$A_0 = \frac{(a_c t + v_0)A_p}{C_D}\sqrt{\frac{\frac{1}{2}\rho A_p}{P_R(A_P - A_R) + W - ma_c - P_e A_p}} \tag{3.28}$$

The cushioning time can be related to cushion position using:

$$x(t) = \frac{1}{2}a_c t^2 + 2v_0 t + x_0 \tag{3.29}$$

where

x(t) is the position of the piston as a function of time,

v_0 is the initial velocity of the piston upon entering the cushioning region, and

x_0 is the displacement position of the piston upon entering the cushioning region, and was defined to be zero.

The position equation was solved for time, t, using the quadratic formula:

$$t = \frac{-2v_0 + \sqrt{4v_0^2 + 8a_c x}}{2a_c} \tag{3.30}$$

which was substituted for t in equation 3.28. This analysis resulted in the relationship of the orifice area between the cushion spear and the sidewall of the cushioning cavity as a

function of insertion depth for constant deceleration with constant supply and exhaust pressures.

The purpose of developing this relationship was to give insight into what cushion spear would ideally result in constant deceleration. In addition, by applying this ideal cushion area-depth relationship to the dynamic model, the resulting velocity profile could be compared against that resulting from constant deceleration and serve as confirmation of the results from the dynamic model. Comparing these results provided confidence in the fidelity of the dynamic model.

Cushion Design Optimization

Using the dynamic model of the cylinder cushioning system, a cushion design optimization procedure was implemented to find the spear dimensions that, for the selected style of spear, would result in a velocity profile that best matched the desired cylinder deceleration performance as specified by the customer. For each spear type, a limited set of geometric dimensions thought to have the greatest effect on cushioning performance were adjusted through optimization (Table 3.1). The dimensions for the first three spears types were defined in Figure 3.7. For the piccolo cushion design, D represents the diameter of the spear, L is the length, t is the wall thickness and p is the diameter of the orifices bored through the wall of the spear (Figure 3.6).

Table 3.1: Spear dimensions varied by the optimization program.

Stepped	Tapered	Parabolic	Piccolo
D1	D1	D1	D
D2	D2	D2	L
D3	D3	D3	t
L1	L1	L1	p
L2	L2		
L3			

A genetic algorithm (GA) was used for cushion design optimization. With this approach, the GA enabled a global search of the design space for the dimensions leading to cushioning velocity profiles that best matched the desired performance characteristics (Coello et al., 2007). Genetic algorithms solve optimization problems based on a process that imitates biological evolution. The GA organizes the problem into a population of individual solutions, each of which is represented by a chromosome composed of the solution parameters. The genetic algorithm evaluates the fitness of each individual solution in the population. With every generation, the population moves toward an optimized solution by combining the chromosomes of individual solutions (breeding) that have a good fitness. To keep the optimizer from being trapped in local minima, mutations are applied at each generation to diversify the search of the solution space.

The dynamic model was embedded into the genetic algorithm, and solution fitness was determined by comparing the resulting velocity profiles to a desired velocity profile generated from user inputs including the initial speed and deceleration time. To compare the simulated velocity profile to the desired profile, the root mean square error (RMSE) was calculated and used as the solution fitness to determine how well the spear dimensions could produce velocity results matching the desired performance. The GA used the resulting mean square error as a fitness function which served as the basis for

generating the next set of dimensions to be simulated. The process repeated until the RMSE of sequential simulations stabilized, and the variation was less than 10^{-6} feet per minute. The population size was 200 individuals, and the mutation rate was 20%.

Experiment Methodology

With the completion of the dynamic model and optimization procedure, numerous tests were run to evaluate the simulated results. The dynamic cushion model was used to simulate the relationship of cushion orifice area to spear depth for constant deceleration. During the development of this relationship, two assumptions were made: the fluid pressure in both ends of the cylinder was constant and viscous effects were neglected. Therefore, to effectively compare the results of the dynamic model to the expected results of the analytically designed cushioning spear, adjustments were made to the system being represented in the dynamic model. To maintain constant fluid pressure, the metering orifices were opened to 0.5 in. To remove the viscous effects, the fluid viscosity was set to zero.

Table 3.2: System parameters entered into the optimization program.

Bore Diameter (in)	5	Final Speed (fpm)	0
Rod Diameter (in)	2	Deceleration Time (s)	1.5
Cushion Cavity Diameter (in)	1	Fluid Density (kg/m^3)	861
Max Spear Length (in)	5	Dynamic Viscosity (Pa-s)	0
Metering Orifice Diameters (in)	0.5	Viscous Damping Coefficient [N/(m/s)]	100

Additionally, the initial velocity of the piston assembly and the required rate of deceleration were specified. Based on the dimensions of the cylinder, the steady state velocity was found to be 34.44 fpm. Therefore, with a final velocity of 0 fpm and a deceleration time of 1.5 seconds, the cushioning deceleration was calculated to be 0.12 m/s^2 or 22.96 $feet/min^2$.

The shape of the spear design generated by the analytical equation cannot be described by any of the spear types common to industry. Thus, tests were run to see whether the constant deceleration response could be replicated with the tapered or parabolic spear types. To calculate the tapered and parabolic spear profiles that would best match the results of the analytical equation, linear and quadratic regression curves were fit to the orifice area-spear depth function. Additionally, to investigate the effect of the assumptions made during the development of the analytical equation, the dimensions of the analytically developed cushioning spear were simulated with viscous effects included.

To investigate how well the commonly-used spear types could achieve a constant deceleration velocity profile, the cushion design optimization was run for each of the four spear shapes using the same system parameters (Table 3.2). The difference between the desired velocity profile and the response produced by the optimized result for each spear type was quantified by calculating the root mean square error (RMSE). The calculated RMSE value serves as a performance metric for the common spear types.

Lastly, the optimization process works by repeatedly running the model while varying spear dimensions (shown in Figure 3.2) such as cushion spear diameter and length. Due to the nature of this process, the optimizer produced different designs each time the process was run. Therefore, the cushion design optimization procedure was run ten times for each of the four cushion spear design types to capture the range of results that the optimizer produced using the system parameters shown in Table 3.2.

Results

Analytical Analysis

By entering the parameters listed in Table 3.2 into equation 3.28, the orifice area required to produce constant deceleration was found along the length of the spear. From this relationship, the necessary spear diameter along the length of the spear was found (Figure 3.8). The diameter profile appeared linear for the first portion of the spear and curved near the end. This observation means that the ideal shape is a mixture of the tapered and parabolic shapes currently used.

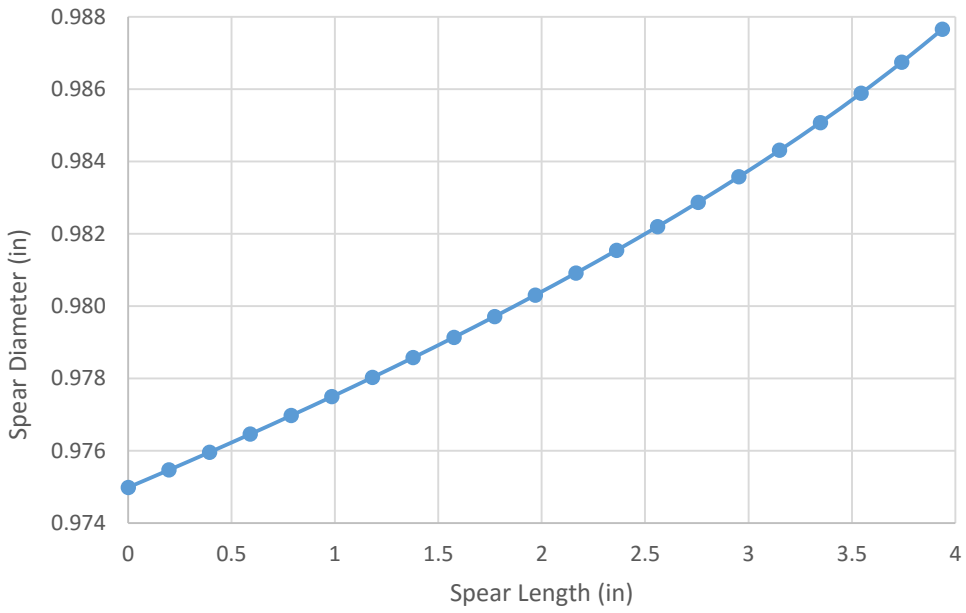

Figure 3.8: Constant deceleration spear design showing spear diameter as a function of length.

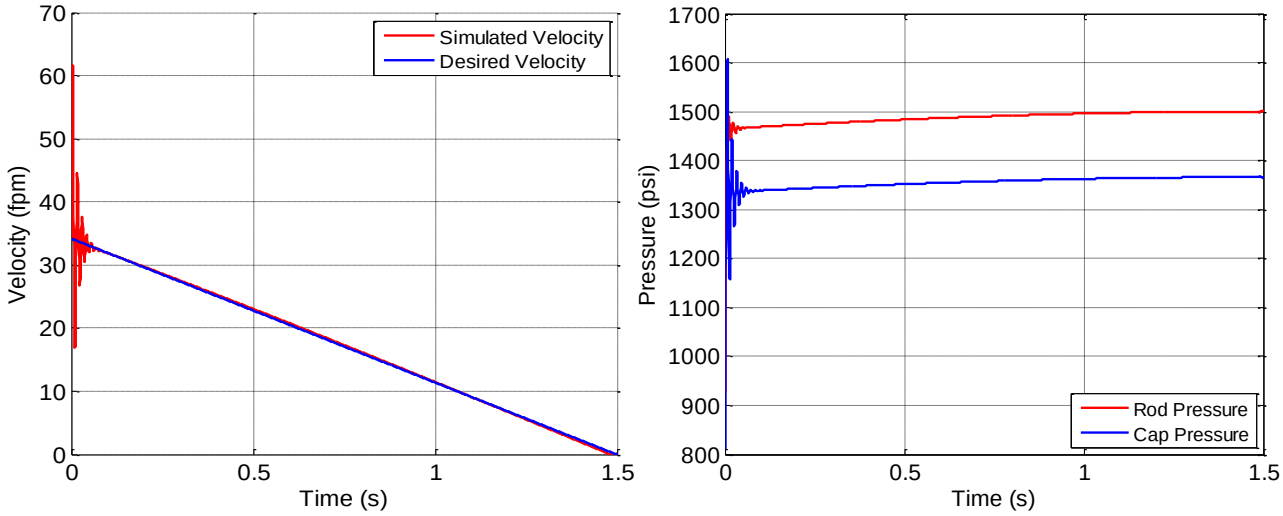

Figure 3.9: Velocity (a) and pressure (b) results of entering the analytically calculated spear profile into the dynamic model.

When this shape was entered into the dynamic model and simulated, the resulting velocity profile matched the desired response very closely (Figure 3.9). The rapid oscillations at the beginning of the cushioning phase were due to the change in the dynamics as the system switches from not being cushioned to additional cushioning resistances being added to the system in a step-like manner. The oscillations represent the interaction between the fluid capacitance and the rod-piston-load mass. The RMSE being the simulated response and the expected response was 1.47 x 10^{-3} m/s (0.29 fpm) which is quite low indicating a good match between the simulation and the design velocity profile.

While the results of running the analytically ideal cushion spear design produced the expected result, the equation used to describe this design does not match with any commonly used spear shapes (Figure 3.2). Therefore, since the parabolic and tapered spear shapes most closely matched the ideal cushion area-spear depth relationship, quadratic and linear regression lines were fit to the relationship. To represent the tapered

spear type, the analytical data was fit with two linear regressions, one from a length of 0 to 65 mm (0 to 2.56 in.) and the other from 65 to 102 mm (2.56 in. to 4 in.). The two resulting lines were used because of the curved nature of the data and because many tapered cushioning spears do have multiple sections with different taper angles along their length. These regression curves fit the ideal relationship with coefficient of determination, R^2, value of 0.998 for both lines (Figure 3.10). The second order polynomial regression resulted in a parabolic spear shape and had an R^2 value of 0.9997 (Figure 3.11).

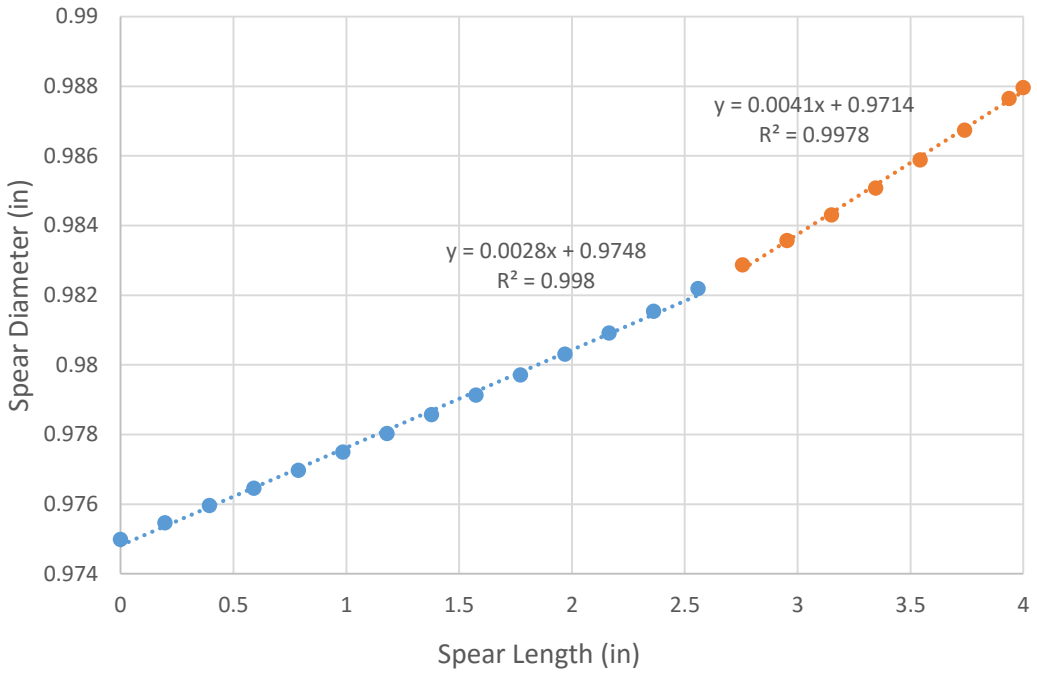

Figure 3.10: Analytical data fit with two linear regression curves.

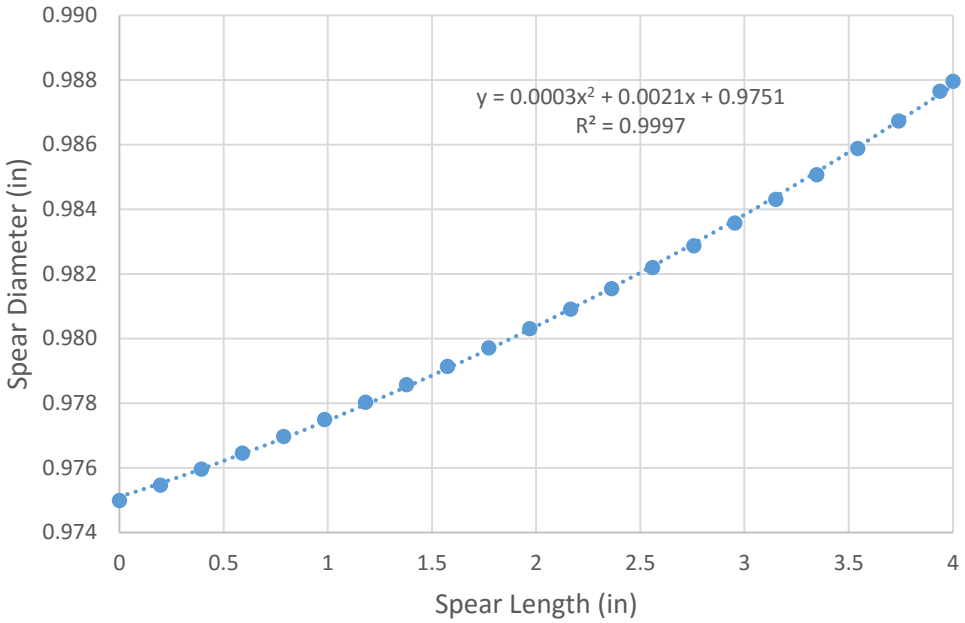

Figure 3.11: Analytical data fit with a quadratic regression curves.

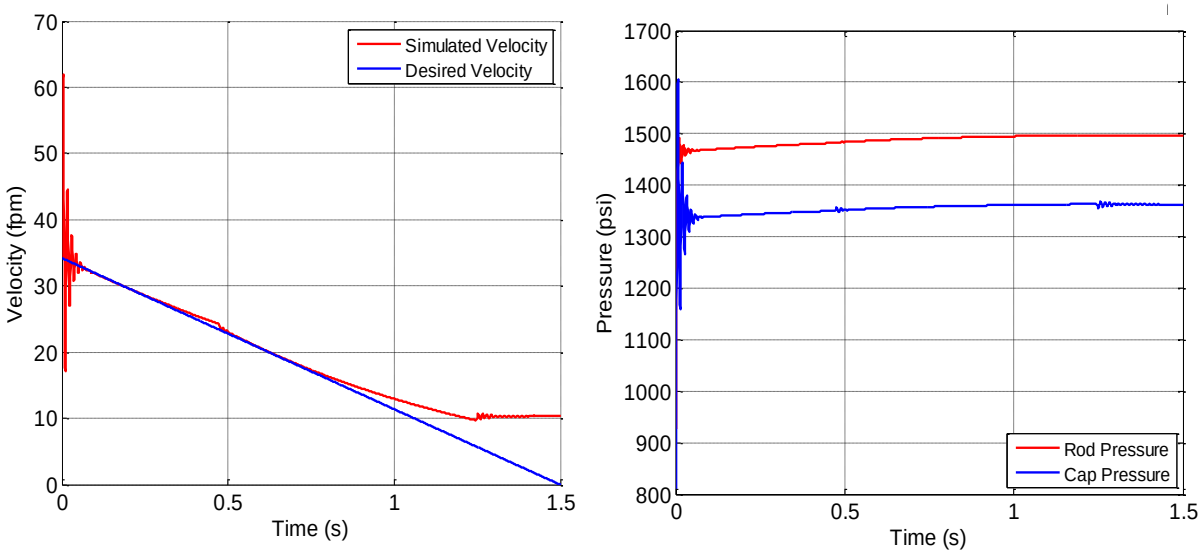

Figure 3.12: Velocity (a) and pressure (b) results of the tapered regression curve fit to analytical data.

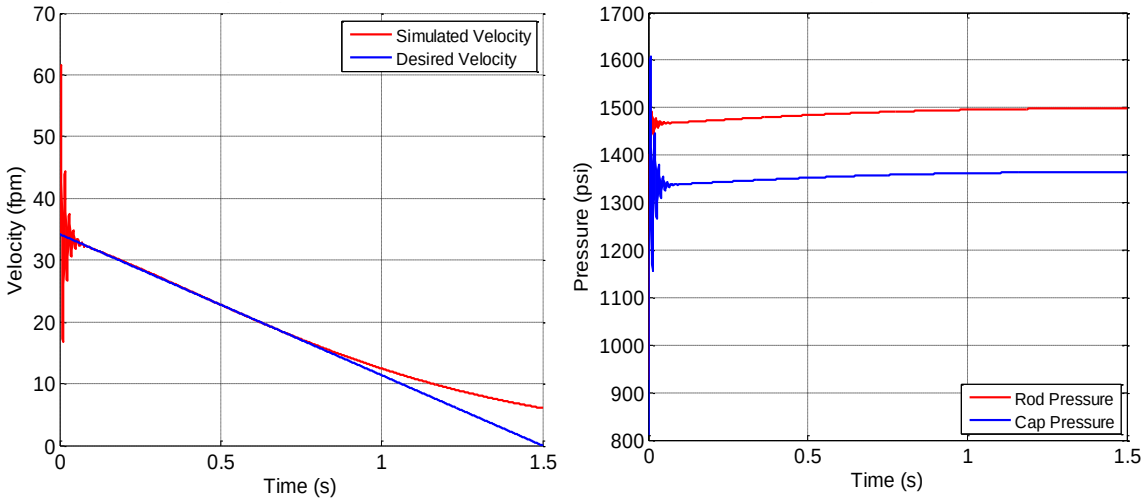

Figure 3.13: Velocity (a) and pressure (b) results of the parabolic regression curve fit to analytical data.

When the dynamic cushion model was simulated with the tapered and parabolic spear shapes arising from the regression curves, the resulting velocity profiles matched the constant deceleration profiles, but with some departure from that observed in the simulations with the ideal relationship. Specifically, in the case of the tapered spear, the simulated velocity profile started to depart from the desire at the end of the first taper segment (as observed at about 0.4 seconds; Figures 3.12) and then near the end of the second segment (as observed at about 0.75 seconds). The start of the flat velocity at about 1.25 seconds signals the end of the cushioning spear. For the parabolic spear, the simulated velocity profile closely matched the desired profile until about 0.75 seconds (Figure 3.13). This type of response in which the deceleration is reduced near the end of the spear is due to the relationship between spear area and flow rate not resulting in sufficient cushion pressure to continue to decelerate piston-rod assembly as desired. The error in the velocity profiles of the tapered and parabolic spears matched the error in the diameter of the spears (Figure 3.14). A positive error means the diameter of the tapered

and parabolic spears was larger than the analytically developed spear and a negative error means that the diameter was smaller.

The simulated velocity profile for the parabolic spear had an RMSE of 14.9×10^{-3} m/s (2.94 fpm) and that of the tapered spear was 21.7×10^{-3} m/s (4.28 fpm). These errors were substantially higher than that of the spear with the ideal shape. The variation in the calculated RMSE value demonstrates the sensitivity of the system to variations in the geometric profile of the cushioning spear, even variations that are less than typical manufacturing tolerances. This means that to truly achieve constant deceleration, manufacturers must take care to keep the spear profile close to the ideal shape and consider the trade-offs between manufacturing tolerances and the need to meet a desired velocity profile.

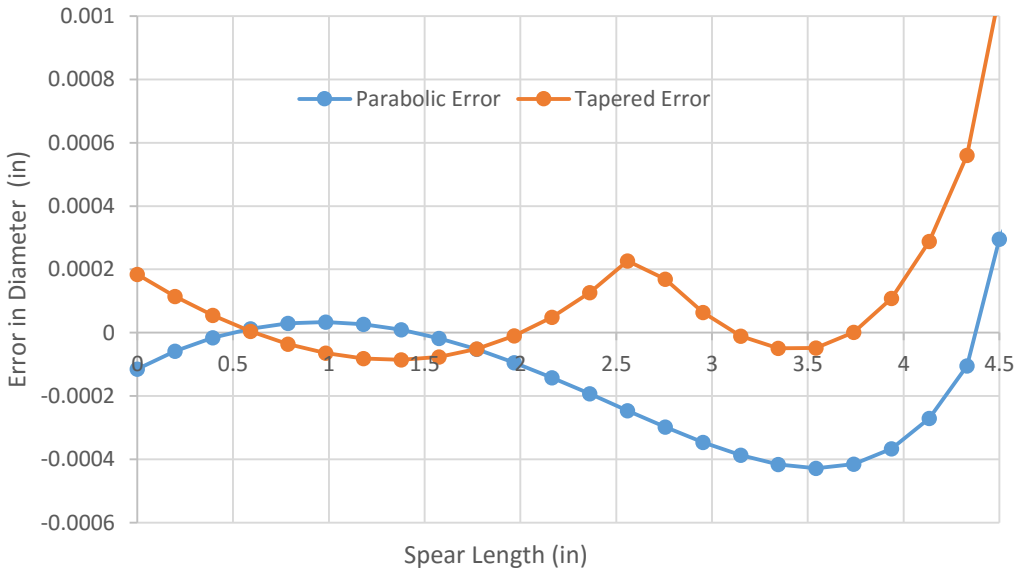

Figure 3.14: Dimensional error between the two spear types developed from the regression fits and the spear type developed analytically.

Achieving the desired results of entering the analytically developed cushion spear into the dynamic model provided confidence in the fidelity of the dynamic model. However, cushioning cannot solely be described by an orifice as was the case with the analytical approach. To increase the fidelity of the model, the viscous effects of laminar flow through the annular clearance was included. When viscous effects were included for a fluid with a viscosity of 47 cP, the simulated velocity profile of the ideal spear shape was no longer linear and the RMSE value increased 41 x 10^{-3} m/s (8.01 fpm; Figure 3.15). The tapered and parabolic spear types performed similarly to the analytically developed curve when viscous effects were included. Therefore, an optimization procedure was employed to select the dimensions of a cushioning spear that, with viscous effects included, would best meet the desired velocity profile.

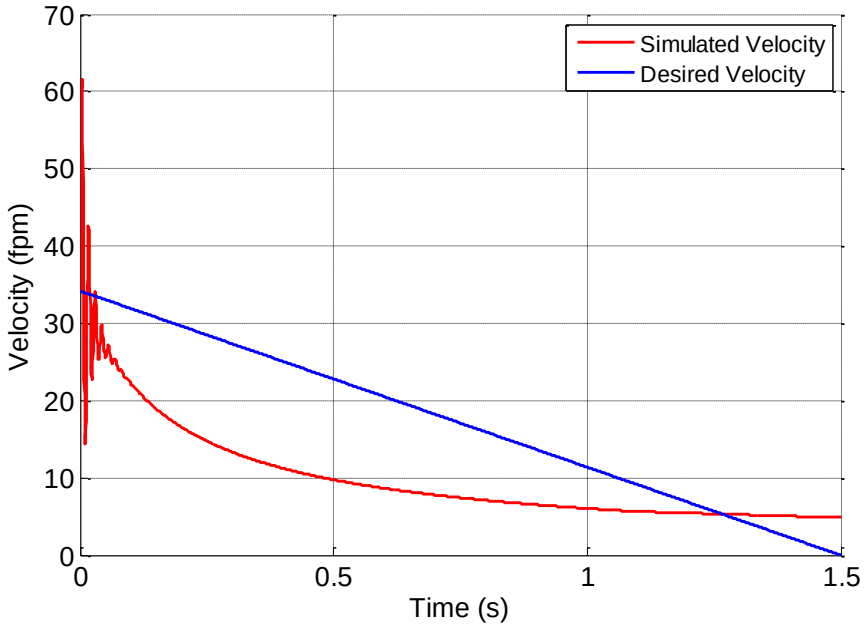

Figure 3.15: Velocity response of the analytically designed cushioning spear with viscous effects included.

Cushion Design Optimization

To analyze and compare the simulated results for multiple spears designs with varied dimensions, the cushion design optimization procedure utilized the RMSE value calculated by measuring the difference between the simulated velocity profile and the desired velocity profile. The calculated error includes a square operation, meaning the calculation does not consider whether the error is located above or below the desired velocity. Because of this effect, the optimizer finds many possible "best" solutions resulting in a family of results that vary between repeated runs. Ten applications of the design optimization procedure to the parabolic spear shape produced RMSE values ranging from 21.4×10^{-3} - 30.8×10^{-3} m/s (4.22-6.06 fpm) with an average error of 25.2×10^{-3} m/s (4.96 fpm) and a standard deviation of 3.2×10^{-3} m/s (0.63 fpm). The solutions tended to fall within a 25.4×10^{-3} m/s (5 fpm) band for most of the cushioning phase (Figure 3.16). Detailed results including the dimensions and RMSE values produced from each of the ten runs are included in the appendix.

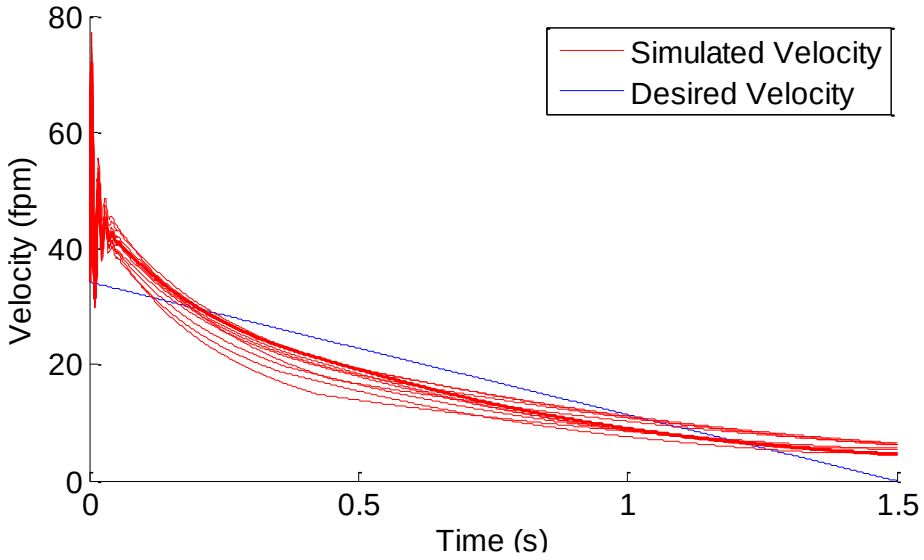

Figure 3.16: Optimized velocity results for a parabolic cushioning spear.

Plotting the results from all ten of the test runs shows the variation in the responses produced by the optimizer; however, to compare the responses of the various spear shapes it is valuable to examine the results of a single run, Figure 3.17. While the velocity profile is not linear, the shape of the response is smooth with the final velocity of the piston reduced by over four times.

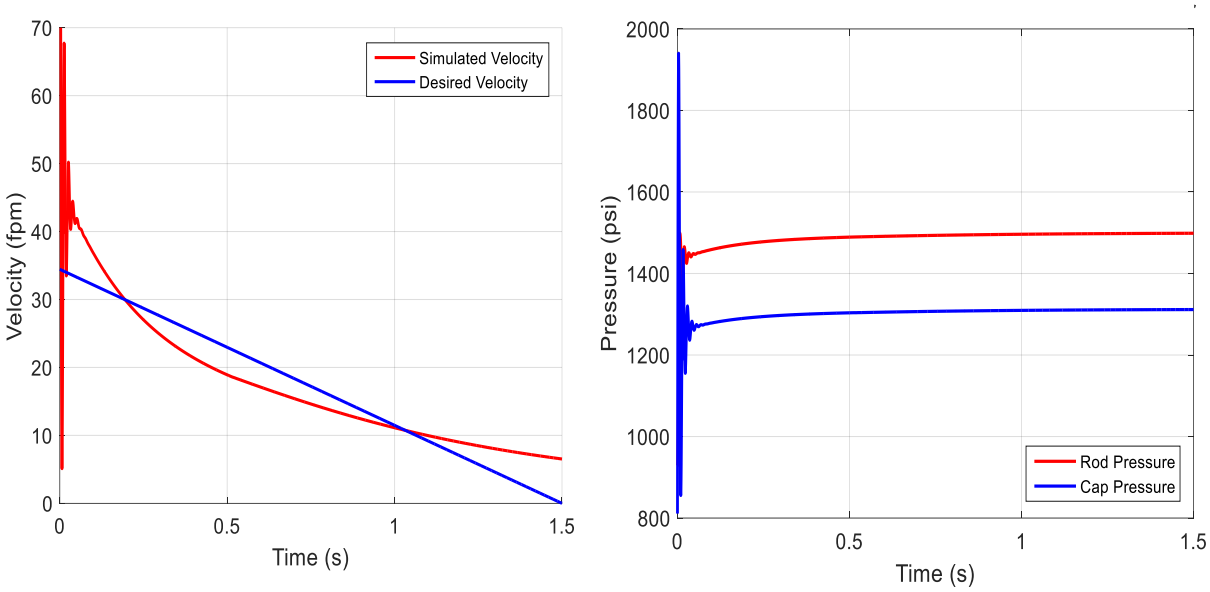

Figure 3.17: The velocity (a) and pressure (b) response of the optimized parabolic profile.

A similar process was conducted for the stepped profile cushion spear type. The RMSE of the resulting velocity profiles ranged from $22x10^{-3}$ – $28x10^{-3}$ m/s (4.35-5.52 fpm) with an average error of $25x10^{-3}$ m/s (4.93 fpm) and a standard deviation of $1.9x10^{-3}$ m/s (0.38 fpm). The location of the sudden drops in velocity caused by the stepped spear shape shifts as the cushion design optimization procedure finds designs with steps of varying length (Figure 3.18).

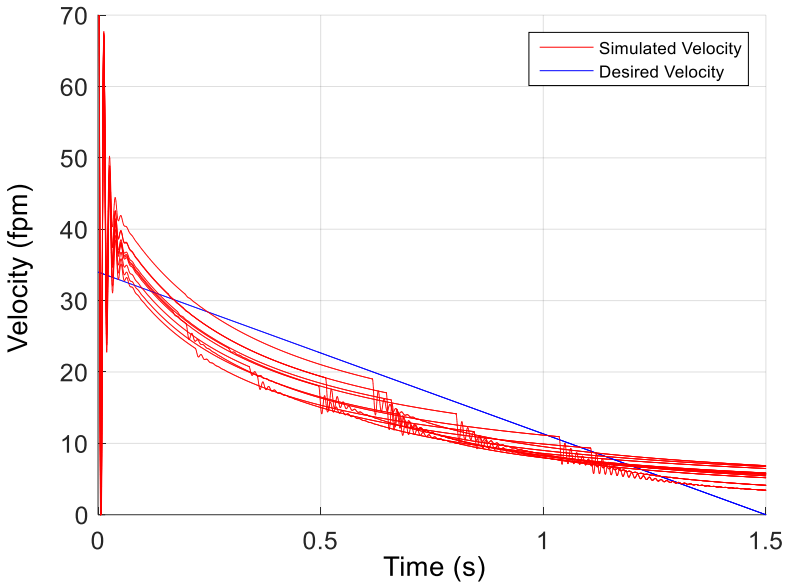

Figure 3.18: Optimized velocity results for a stepped cushioning spear.

In analyzing the response of a single run, the differences between the spear types become more obvious. Sudden changes in the diameter of the stepped spear shape lead to points along the velocity response where the piston speed drops abruptly, Figure 3.19. The velocity reduction upon the start of cushioning is more pronounced because the design optimizer selected spear dimensions with larger starting diameters when compared to the parabolic and tapered spear types.

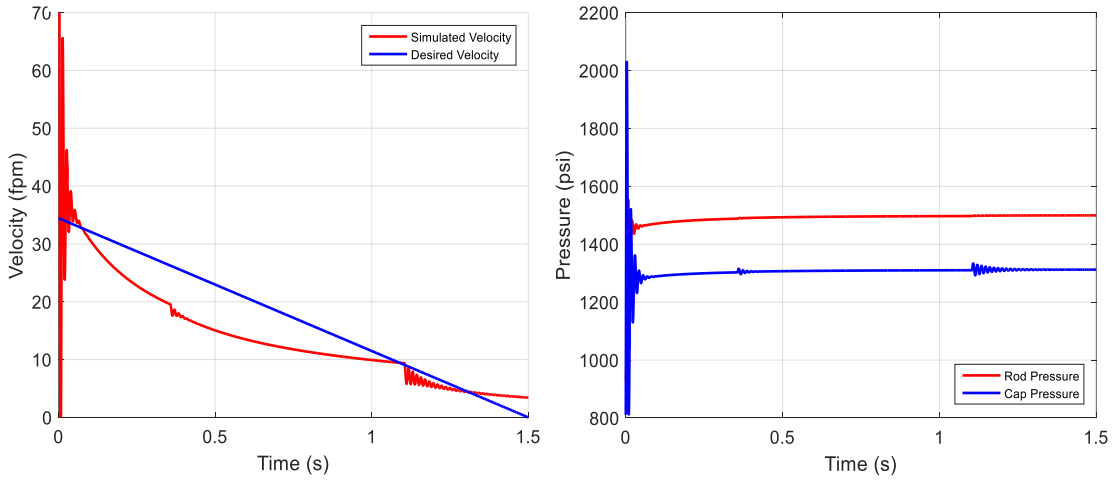

Figure 3.19: The velocity (a) and pressure (b) response of the optimized stepped profile.

When optimization was performed with the tapered cushion, the resulting velocity profiles were more consistent than those observed with the other cushion types (Figure 3.20). The resulting velocity profiles had RMSE ranging from $22.9x10^{-3}$ – $26.9x10^{-3}$ m/s (4.51-5.31 fpm) with the average error being $24.4x10^{-3}$ m/s (4.81 fpm) and a standard deviation of $1x10^{-3}$ m/s (0.20 fpm).

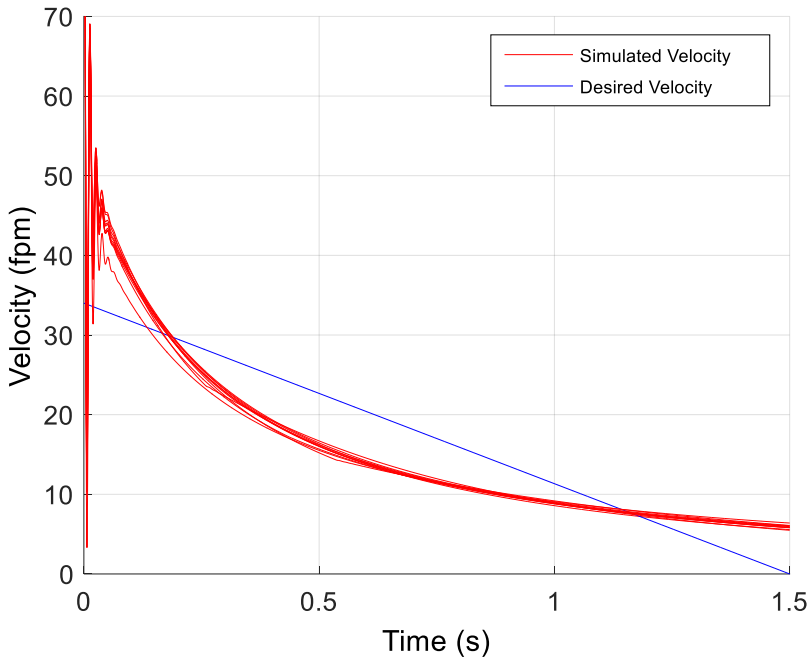

Figure 3.20: Optimized velocity results for a tapered cushioning spear.

The tapered and parabolic spear types produced responses with very similar, smooth shapes. However, the results of the tapered spear indicate that the piston decelerates faster and deviates further from the desired velocity profile when compared to the parabolic spear, Figure 3.21.

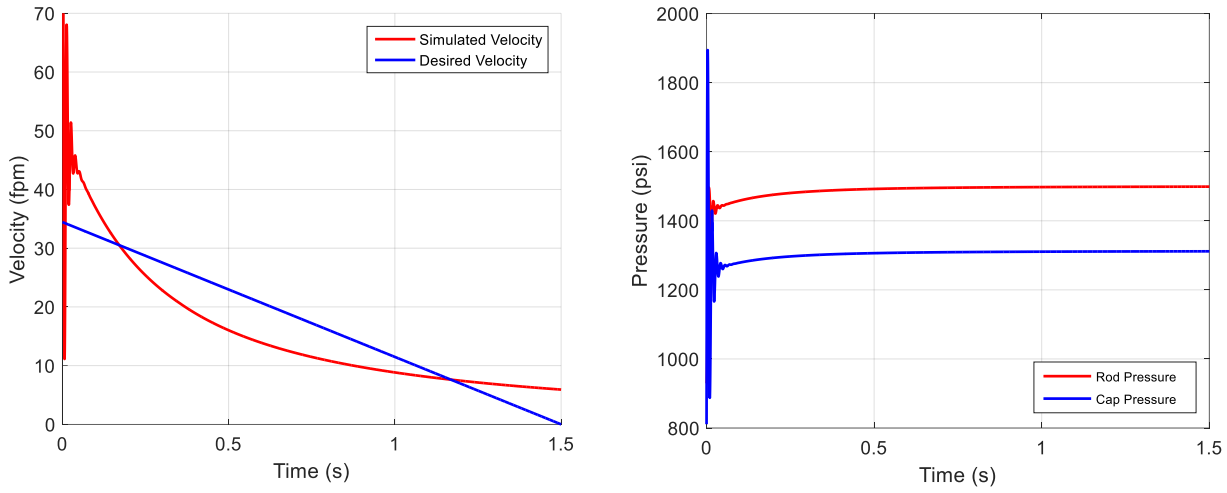

Figure 3.21: The velocity (a) and pressure (b) response of the optimized tapered profile.

Lastly, the piccolo style spear produced results similar to the stepped spear (Figure 3.22), but with substantantially more error and variation in error. The RMSE values ranged from 22.4×10^{-3} - 33.6×10^{-3} m/s (4.41-6.61 fpm) with an average error of 25.8×10^{-3} m/s (5.07 fpm) and a standard deviation of 3.7×10^{-3} m/s (0.73 fpm).

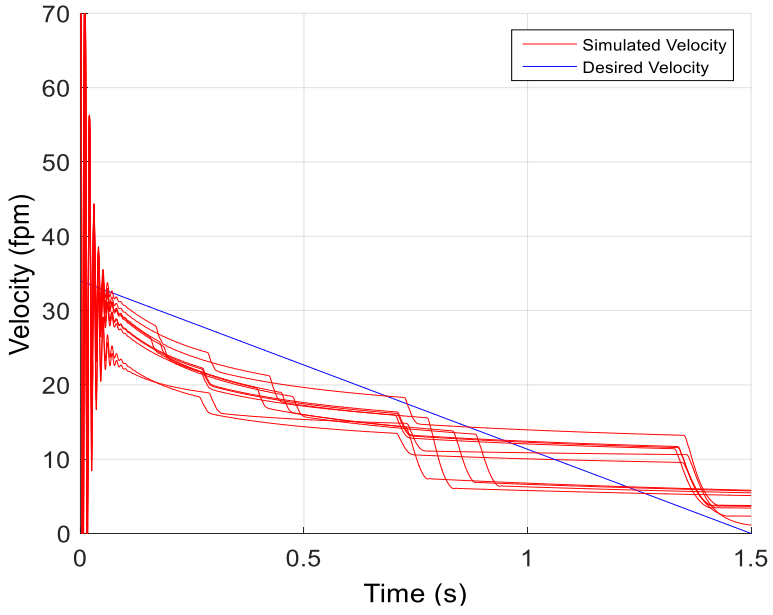

Figure 3.22: Optimized velocity results for a piccolo shaped cushioning spear.

The velocity and pressure results of the piccolo profile were similar to those associated with the stepped spear shape, Figure 3.23. The sudden drop in velocity occurred as each of the piccolo holes were cut off.

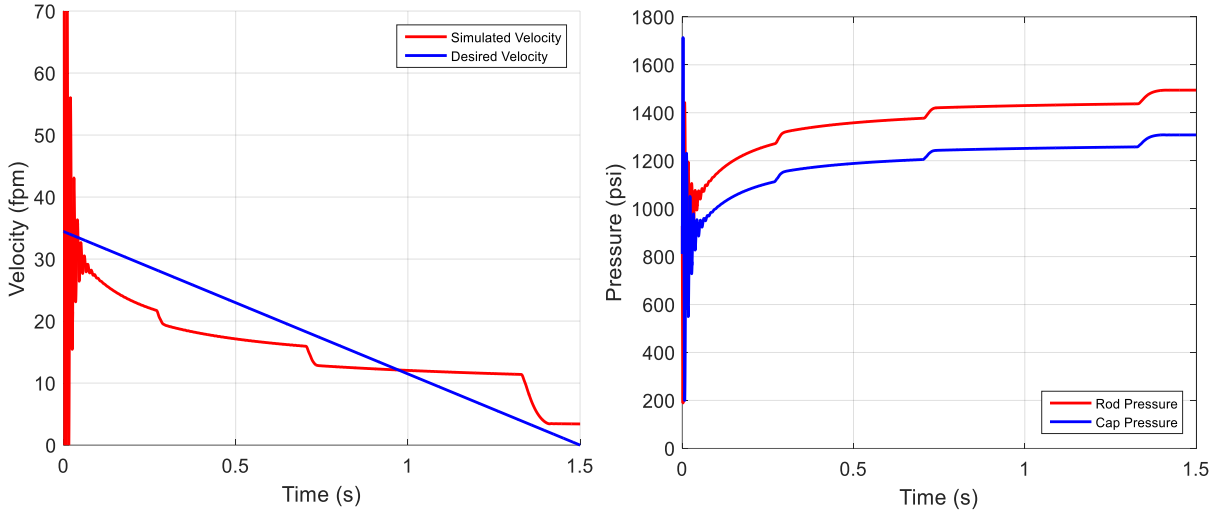

Figure 3.23: The velocity (a) and pressure (b) response of the optimized piccolo profile.

The calculated RMSE values for the four optimized spear types, the analytically produced spear geometry and the two regression curves are compared in Table 3.3. The optimized spear types include viscous effects while the analytical spear along with the parabolic and tapered approximations do not include viscous effects. The results indicate that the effects of including a viscous fluid of cushioning were represented in the size of the error between the simulated velocity profile and the desired velocity profile.

Table 3.3: RMSE values for the various spear types tested

Spear Type	RMSE (fpm)	Standard Deviation (fpm)
Stepped	4.93	0.38
Tapered	4.81	0.20
Parabolic	4.96	0.63
Piccolo	5.12	0.75
Analytically Developed Cushion	0.29	-
Tapered Fit to Analytical Curve	4.28	-
Parabolic Fit to Analytical Curve	2.94	-

Conclusions

From the results of this research, it can be concluded that:

1. Spear profile produced by the analytical model to achieve constant deceleration results in simulated cushion velocity results representing nearly constant deceleration based the dynamic model of the cushion system. The correspondence between the two approaches lends credibility to the fidelity of the dynamic cushion model.
2. By neglecting the viscous effects during the development of the analytical equation, the system being modeled does not fully capture the effects of cushioning.
3. The profile produced by the analytical analysis was a mixture of two common spear types with the first part representative of a tapered spear while the second portion was more similar to a parabolic spear. When the results of the analytical analysis were fit with more common tapered or parabolic curves, the resulting velocity responses deviated from constant deceleration responses. Therefore, the velocity response of the cushioning spears is highly sensitive to changes in the spear profile.
4. Under conditions where the pressures in each end of the cylinder were held constant, the four common spear types performed very similarly. The main difference indicated by the results was that the parabolic and tapered spear types produce smoother velocity profiles.

5. The results of the optimization tests demonstrated that the optimization procedure was effective in selecting spear shapes that most closely follow the desired velocity profile.

The results of this project have potential to impact manufacturers of cylinders with cushions. Where previous cushion designs were based on a more time consuming iterative process done by the designer, this dynamic modelling approach and cushion design optimization procedure can enhance the design process by providing more information to the designer and their customers. Also, with the sophistication of modern manufacturing equipment, it is possible to manufacture the new cushion designs developed using the approach.

References

Anon. "Constant deceleration cylinder has special built-in shock absorber", *Product Engineering* (1973).

Anon. “Modeling of hydraulic systems”, *Modelon AB* (2013).

Chen, Xun, Jun Zhou, Lihong Li, and Yanliang Zhang. "Cushioning structure optimization of excavator arm cylinder." *Automation in Construction* 53 (2015): 120-30.

Chengbin, Wang, and Quan Long. "Study on simulation and experiment of hydraulic excavator's work device based on Simulation X." *International Conference on Electric Information and Control Engineering, 15-17 April 2011*.

Coello, Carlos A., Gary B. Lamont, and David A. Van Veldhuizen. *Evolutionary Algorithms for Solving Multi-Objective Problems*. 2nd ed. New York: Springer, 2007.

Esposito, A. *Fluid Power with Applications* (6th ed.). Upper Saddle River, N.J.: Prentice Hall, (2003).

Green, W. L. "Cushioning for hydraulic cylinders." *Hydraulics & Pneumatics* (1968): 100-04.

Manring, Noah D. *Hydraulic Control Systems*. New York: Wiley, (2005).

Merritt, H. *Hydraulic Control Systems*. New York: Wiley, (1967).

Norvelle, F. *Fluid Power Technology*. Minneapolis/St. Paul: West Pub, (1995).

Schwartz, C., V. J. De Negri, and J. V. Climaco. "Modeling and analysis of an auto-adjustable stroke end cushioning device for hydraulic cylinders." *J. Braz. Soc. Mech. Sci. Eng.* 27.4 (2005): 415-25.

Shampine, L. F. and M. W. Reichelt, "The MATLAB ODE suite." *SIAM Journal on Scientific Computing*, Vol. 18, 1997, pp. 1–22.

Thorner, Frank. *Investigation of Hydraulic Cylinder Cushioning.* Sheffield Hallam University, (1998).

CHAPTER 4. GENERAL CONCLUSIONS AND SUGGESTED WORK

From the results obtained from this research, the following general conclusions were drawn:

1) Dynamic modeling of the cylinder cushion dynamics with associated insights have the potential to make an impact on cylinder manufacturers which have design scenarios where cylinder cushioning and cushion performance is important. Where previous cushion designs were based on design rules-of-thumb and trial-and-error, the use of dynamic models and simulation can save time, effort, and money.
2) The results of simulating the analytically developed cushion spear matched what was expected, thus providing confidence in the results of the dynamic model.
3) The dynamic modeling and simulation of cushions resulted in velocity and pressure profiles that can provide insight to designers and their customers.
4) Cushion design optimization was effective in selecting spear shapes that most closely follow the desired velocity profile even with the additional fidelity associated with models of laminar flow though the annular clearance between the cushion spear and cushion cavity side wall.

The following items are suggested for future research that would build upon this project:

1) Future research should focus on the development of the spear shape produced through the analytical analysis. While the current analysis requires the assumption of constant system pressures and a non-viscous fluid, further research could

develop an equation that can compensate for fluctuating pressures in the system and include the viscous effects that proved to be essential.

2) A sensitivity analysis should be performed to identify which of the cushioning spear dimensions has the largest impact on the velocity and pressure response.

APPENDIX-DETAILED RESULTS OF DESIGN OPTIMIZATION PROCEDURE

Full results of running the optimizer ten times for each spear type. Dimensions are in inches, error values and statistical results are in feet per minute.

Stepped	D1	D2	D3	L1	L2	L3	RMSE	Average
1	0.9667	0.9671	0.9774	1.1808	1.4615	1.9387	4.5977	3.88522
2	0.9678	0.9703	0.9868	1.9529	1.9895	1.3703	3.3611	**Std Dev**
3	0.9669	0.9696	0.9803	1.3426	1.76	1.4444	4.346	0.4461
4	0.9693	0.9708	0.9824	1.3326	1.9501	1.7616	4.418	
5	0.9662	0.9665	0.98	1.2618	1.9923	1.6401	3.7893	
6	0.9686	0.973	0.989	1.9627	1.8763	1.5117	3.8494	
7	0.9651	0.9653	0.9802	1.3816	1.9815	1.3788	3.6171	
8	0.9631	0.9633	0.9774	1.495	1.9999	1.9353	3.4064	
9	0.9665	0.9673	0.9819	1.838	1.8056	1.3602	3.3129	
10	0.965	0.9653	0.9769	1.1847	1.6885	1.7241	4.1543	
Tapered	**D1**	**D2**	**D3**	**L1**	**L2**		**RMSE**	**Average**
1	0.958662	0.972051	0.987304	2.633086	2.96766		4.2448	4.29468
2	0.960547	0.96828	0.981781	2.998226	2.242537		4.1561	**Std Dev**
3	0.955986	0.975014	0.979235	1.86028	2.894139		3.9711	0.1791
4	0.959503	0.975597	0.985813	2.537318	2.992697		4.4173	
5	0.958726	0.975782	0.9879	2.939935	2.93439		4.2652	
6	0.960879	0.966813	0.985897	2.720684	2.987006		4.23	
7	0.956208	0.982711	0.987917	2.928572	2.872868		4.5334	
8	0.958839	0.972095	0.983382	2.196777	2.962114		4.212	
9	0.960372	0.969106	0.982863	2.26153	2.698748		4.2899	
10	0.964018	0.970932	0.98184	2.920587	2.425566		4.627	
Parabolic	**D1**	**D2**	**D3**	**L1**			**RMSE**	**Average**
1	0.9650	0.97	0.986	4.378			4.0422	3.7429
2	0.962392	0.967013	0.98989	5.921584			3.1861	**Std Dev**
3	0.96569	0.971378	0.988025	4.070084			4.5233	0.6983
4	0.963291	0.976112	0.989864	4.475033			5.2846	
5	0.965089	0.966156	0.988594	4.901842			3.1612	
6	0.963513	0.966658	0.988495	5.927051			3.3371	
7	0.959845	0.972443	0.989362	5.408715			4.0253	
8	0.964556	0.968138	0.989919	5.86767			3.6534	
9	0.965915	0.967058	0.989703	4.927755			3.3245	
10	0.965076	0.96509	0.989953	5.189492			2.8913	

Piccolo	D	L	t	p			RMSE	Average
1	0.9820	5.0725	0.3195	0.1015			6.6082	5.07266
2	0.9779	5.9823	0.4781	0.1051			4.8229	**Std Dev**
3	0.9751	4.0759	0.7869	0.1014			5.3530	0.7251
4	0.9784	5.9631	0.8720	0.1071			4.8059	
5	0.9775	6.1049	0.3813	0.1059			4.6324	
6	0.9749	4.5265	0.6831	0.1012			4.6760	
7	0.9776	6.1570	0.7059	0.1076			4.5758	
8	0.9858	5.3671	0.1142	0.1167			6.2600	
9	0.9758	4.6144	0.3327	0.1192			4.4075	
10	0.9753	4.6662	0.8395	0.1012			4.5849	